| OF |
AD
A052 716

AD A052716

RADC-TR-78-21
Interim Report
March 1978

ADVANCED MULTI-MODE TWT

Louis Lau

Teledyne MEC

D D C
RECEIVED
APR 17 1978
F

Approved for public release; distribution unlimited.

ROME AIR DEVELOPMENT CENTER
Air Force Systems Command
Griffiss Air Force Base, New York 13441

This report has been reviewed by the RADC Information Office (OI) and is releasable to the National Technical Information Service (NTIS). At NTIS it will be releasable to the general public, including foreign nations.

RADC-TR-78-21 has been reviewed and is approved for publication.

APPROVED: *Dirk T Bussey*

DIRK T. BUSSEY
Project Engineer

APPROVED: *Joseph L Ryerson*

JOSEPH L. RYERSON
Technical Director
Surveillance Division

FOR THE COMMANDER: *John P. Huss*

JOHN P. HUSS
Acting Chief, Plans Office

If your address has changed or if you wish to be removed from the RADC mailing list, or if the addressee is no longer employed by your organization, please notify RADC (OCTP) Griffiss AFB NY 13441. This will assist us in maintaining a current mailing list.

Do not return this copy. Retain or destroy.

SECURITY CLASSIFICATION OF THIS PAGE *(When Data Entered)*

REPORT DOCUMENTATION PAGE		READ INSTRUCTIONS BEFORE COMPLETING FORM
1. REPORT NUMBER RADC-TR-78-21	2. GOVT ACCESSION NO.	3. RECIPIENT'S CATALOG NUMBER
4. TITLE *(and Subtitle)* ADVANCED MULTI-MODE TWT		5. TYPE OF REPORT & PERIOD COVERED Interim Report. 24 Sep 76 – 30 Jun 77 6. PERFORMING ORG. REPORT NUMBER N/A
7. AUTHOR(s) Louis Lau		8. CONTRACT OR GRANT NUMBER(s) F30602-76-C-0406
9. PERFORMING ORGANIZATION NAME AND ADDRESS Teledyne MEC 3165 Porter Drive Palo Alto CA 94304		10. PROGRAM ELEMENT, PROJECT, TASK AREA & WORK UNIT NUMBERS 62702F 55730207
11. CONTROLLING OFFICE NAME AND ADDRESS Rome Air Development Center (OCTP) Griffiss AFB NY 13441		12. REPORT DATE March 1978 13. NUMBER OF PAGES 50
14. MONITORING AGENCY NAME & ADDRESS*(if different from Controlling Office)* Same		15. SECURITY CLASS. *(of this report)* UNCLASSIFIED 15a. DECLASSIFICATION/DOWNGRADING SCHEDULE N/A

16. DISTRIBUTION STATEMENT *(of this Report)*

Approved for public release; distribution unlimited.

17. DISTRIBUTION STATEMENT *(of the abstract entered in Block 20, if different from Report)*

Same

18. SUPPLEMENTARY NOTES
RADC Project Engineer: Dirk T. Bussey (OCTP)

19. KEY WORDS *(Continue on reverse side if necessary and identify by block number)*

Microwave Tubes

20. ABSTRACT *(Continue on reverse side if necessary and identify by block number)*

Teledyne MEC's Advanced Multi-Mode TWT development program is aimed at achieving 5 dB pulsed performance in an octave-band traveling-wave tube by operating at a reduced drive level in the CW mode and recovering the loss of basic efficiency through the use of a multiple-stage depressed collector.

This report discusses the design approach and progress during the first nine months of the program.

DD FORM 1473 1 JAN 73   EDITION OF 1 NOV 65 IS OBSOLETE

405 649

LB

CONTENTS

ACCESSION for

NTIS	White Section
DDC	Buff Section
UNANNOUNCED	
JUSTIFICATION	

BY
DISTRIBUTION/AVAILABILITY CODES

Di		SPECIAL
A		

iii

Preceding Page BLANK

ILLUSTRATIONS

1.0   PROGRAM GOALS

This report covers the first nine months of a two-year development effort in which a relatively new concept for obtaining dual mode performance from a traveling-wave tube is being investigated.

Dual mode TWT's currently entering production exhibit approximately 3 dB pulse-up over an octave bandwidth. Attempts to achieve higher power pulse-up ratios have been frustrated by poor CW mode efficiency and pulse mode oscillations.

There are several fundamental reasons for power pulse-up limitations which should be reviewed in order to place the current program in perspective. If one examines a TWT designed for octave-band CW mode performance with relatively high basic efficiency, a key requirement is that gain beyond the sever at the band edges be greater than 26 to 28 dB; otherwise, a substantial reduction in basic efficiency will result. However, if a dual mode tube designed to achieve the proper output gain at the band edges in the CW mode is then operated in the pulse mode, where the current in the beam is increased by greater than a factor of 2, gain in the output section at the middle of the band will be on the order of 36 dB, which is equal to the maximum gain which can be obtained in a standard, uniform helix circuit without backward-wave oscillation.

Conversely, if the tube is designed so that gain at the center of the band in P mode is below 36 dB, then reducing the beam current for CW mode operation will no longer produce the required gain in the output section at the band edges.

The program described in this report addresses the problem with a completely different design approach. Rather than altering beam or circuit characteristics to achieve a higher pulsed current, this program began by working within the present guideline of an attainable 3 dB.pulse. An additional 2 dB pulse will be achieved by operating 2 dB down from saturation in the CW mode. By operating the tube at a reduced drive level in the CW mode, a 5 dB power pulse-up ratio can easily be obtained.

-1-

Efficiency can be maintained by the use of a three-stage multiple depressed collector. When the tube is operated that far below saturation, the velocity distribution in the spent beam is greatly reduced and a large amount of the beam current can therefore be collected at a very low potential. Two higher voltage stages will be designed primarily to accommodate the spent beam in the pulse mode.

The goal of this program is to illustrate the feasibility of this concept and to build and deliver three devices which demonstrate these performance goals. The specific performance goals are outlined in the following table:

Performance Parameter	Value
Frequency	f_1 to f_2
CW Mode	
Power Output	P_c minimum
Overall Efficiency	20% minimum
Gain at Rated Power	31 dB
Pulse Mode	
Power Output	P_p minimum
Overall Efficiency	20% minimum
Gain at Rated Power	40 dB minimum
Duty	40% minimum
Parameters for Both Modes:	
VSWR (in band)	1.5:1
VSWR (out of band)	3:1
Cooling	Air Cooled
Focusing	PPM

2.0 BASIC APPROACH

The electron gun and unifilar helix circuit design of this tube (designated the MTZ-6005) is a direct scaling of an existing pulse-up TWT (M5838) used in a current production system. The M5838 operates over approximately the same frequency range as desired in the MTZ-6005. The key difference between the two tubes is the required power level.

The present M5838 operates at a helix voltage of 9600 volts, has a gun perveance in the pulse mode of 0.56 micropervs, and is focused with an Alnico-8 PPM stack. This tube provides an overall efficiency of 18%, operating at approximately half the power output of the desired tube.

Scaling of the M5838 to the higher power requirement at constant gun perveance produced a scaling factor of 1.07, which translates into an operating voltage of 13,000 volts. The parameters of the two tubes are listed in Table I.

TABLE I

Parameter	M5838	MTZ-6005
Helix Voltage	9600–9800 V	12,700–13,300 V
Helix Current		
CW Mode	20 mA	10 mA
Pulse Mode (Peak)	40 mA	20 mA
Helix Current Cutoff	30 mA	35 mA
Collector Voltages (with respect to cathode)		
Stage 1	55% E_w	65% E_w
Stage 2	42% E_w	35% E_w
Stage 3	N/A	12% to 20% E_w
Cathode Current		
CW Mode	330 mA	675 mA
Pulse Mode	465 mA	795 mA
Collector Efficiency		
CW Mode	58%	83%
Pulse Mode	66%	52%
Grid Voltage		
CW Mode	–100 to –190	–135 to –260
Pulse Mode	0 to –35	0 to –50
Cutoff Mode	–1000 max.	–1400 max
Heater Voltage	6.3 V nom.	6.3 V nom.
Heater Current	2.0 A max.	2.0 A max.

3.0 TUBE DESIGN AND PROGRESS

3.1 Circuit Design

Two circuit design efforts were planned for the program. The first, circuit design A, was a simple voltage scaling of the current M5838 tube, undertaken to provide relatively fast results and enable evaluation of some refinements to increase efficiency and to reduce the tendency to backward-wave oscillate. The second effort, circuit design B, was an exact photographic scaling of the M5838 tube, which has a relatively good frequency response over the band in question. It is expected that circuit design B will provide the final design, since design A utilizes the same barrel diameter as the present tube and approximately the same size rods and helix diameters. A slight frequency shift is anticipated in this design, since no dimensions are being changed except the voltage.

The first circuits were designed and cold tested, with the results shown in Figures 1 and 2. Figure 1 illustrates the phase velocity of both the input and output sections of the circuit after scaling. Figure 2 illustrates the axial impedance for the circuit configurations.

One of the key problems to be addressed in the circuit design was that of eliminating backward-wave oscillations, since they were a problem in the production version of this tube and any increase in helix voltage would push this circuit beyond the safety limit. The tendency to oscillate can be reduced by stepping helix velocity. However, a problem arising from this change in velocity is that obtaining the correct synchronous velocity conditions for BWO suppression often compromises forward-wave amplification. This can be alleviated to some degree by changing helix diameter at the point at which the velocity step occurs. This diameter step was incorporated into circuit design A. A velocity profile illustrating the circuit velocity and loss pattern versus actual distance is shown for the first design in Figure 3.
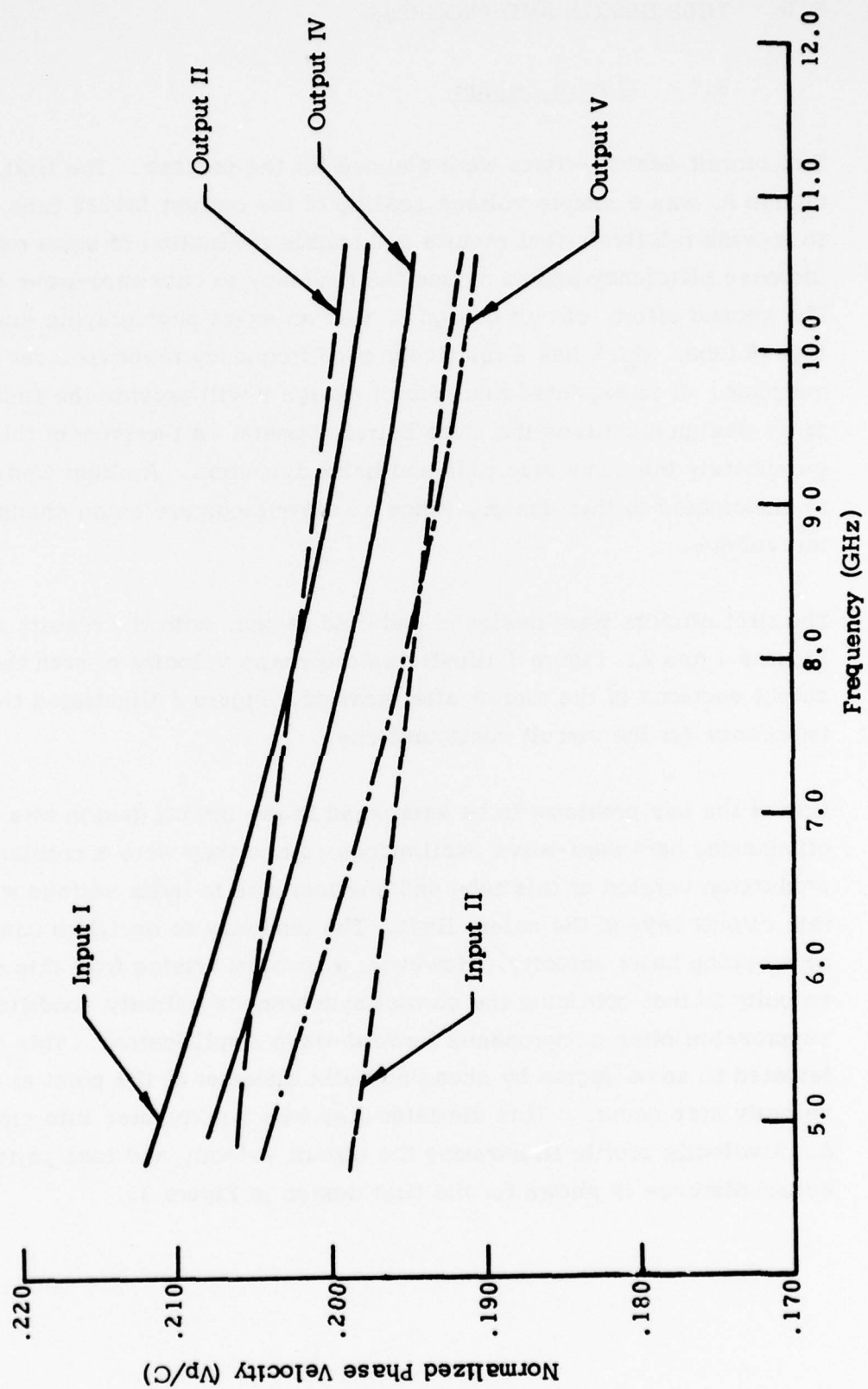
Figure 1. Normalized phase velocity, Design A.
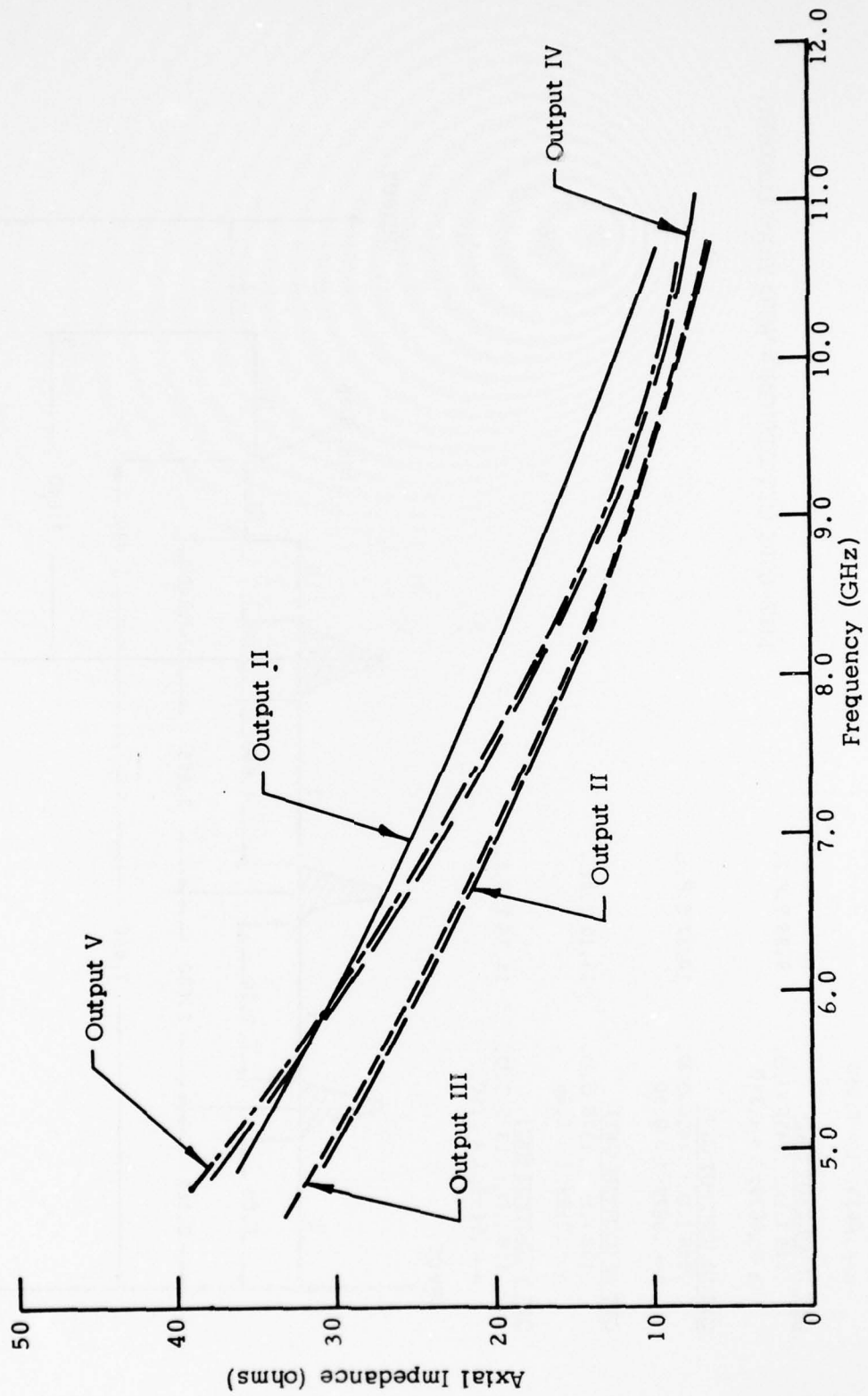
Figure 2. Axial Impedance, Design A.

MTZ-6005 CKT DESIGN A W/O VANE LOADING

CKT I (INPUT CKT)
.118 I.D.; .1376 O.D.
a = .0639; L = 7.660   10.94 T.P.I.

CKT II (OUTPUT CKT)
.126 I.D.; .1456 O.D.
a = .0679; L = 1.340   9.98 T.P.I.

CKT III (OUTPUT CKT)
.126 I.D.; .1456 O.D.
a = .0679; L = 0.50   10.37 T.P.I.

CKT IV (OUTPUT CKT)
.118 I.D.; .1376 O.D.
a = .0639; L = 1.80   11.12 T.P.I.

CKT V (OUTPUT CKT)
.118 I.D.; .1376 O.D.
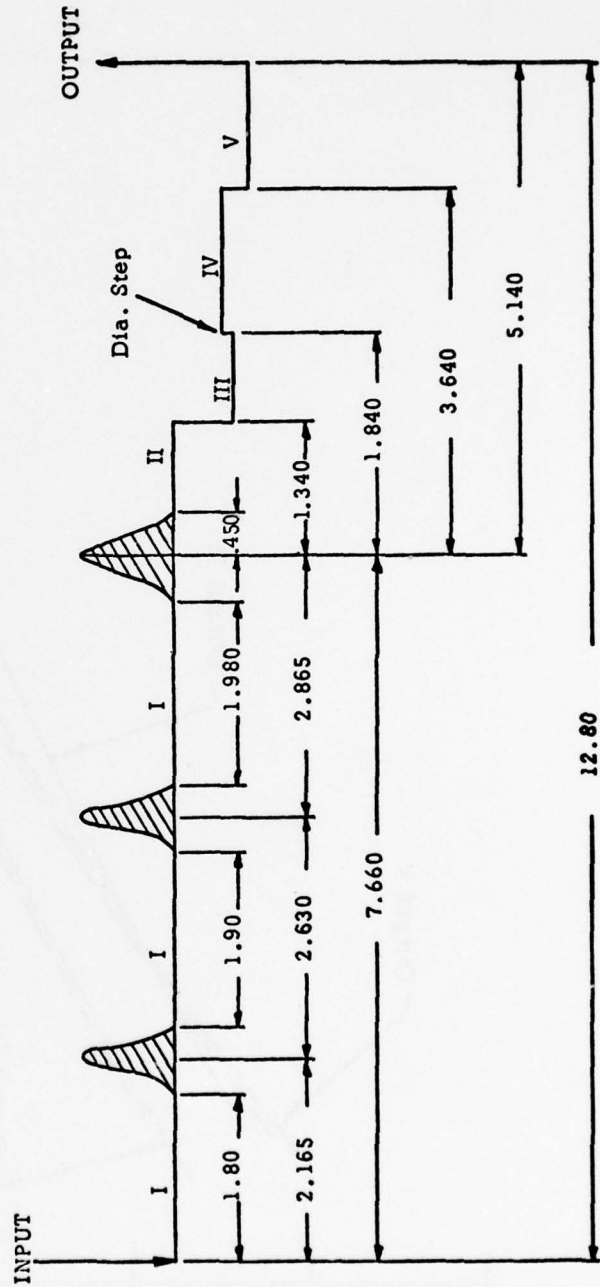a = .0639; L = 1.50   11.34 T.P.I.

INPUT

OUTPUT

Dia. Step

I   I   I   II   III   IV   V

1.80   1.90   1.980   .450

2.165   2.630   2.865   1.340

7.660   1.840

3.640

5.140

12.80

Figure 3. Circuit velocity profile, Model A.

-8-

Circuit B was designed to take advantage of the excellent frequency response of the current tube through a photographic scaling, with all circuit components scaled by a factor of 1.07. Performance of the device using this approach should be the same as in the M5838 tube but at a higher power level. The drawback to this approach is the relatively long lead time required for obtaining special helix support rods and barrels. Table II compares the various circuit design conditions of the two circuits. As a supplement to this table, Figure 4 illustrates the phase velocity of both the input and output sections of circuit design B, and Figure 5 illustrates the axial impedance for this design.

Additional circuit studies using vane loading of the output section of both designs have been conducted in the event that alteration of velocity dispersion over the band becomes necessary. The results of the vane loading for circuit designs A and B are shown in Figures 6 and 7 respectively.

Using the measured results of the phase velocities and interaction impedance, detailed large- and small-computer analyses were conducted on the two circuit designs. The results of these analyses for optimum cases are shown in Figures 8 and 9, which give results for designs A and B respectively. In both cases, performance in the pulse mode is adequately predicted.

3.2 Gun Design

The gun design becomes an important consideration in any new tube design or scaling of an existing design. In both circuit designs A and B, the helix diameter has been increased approximately 7%. The M5838 electron gun has been redesigned using a scaling factor of 1.07. By rescaling the gun, we can maintain the same excellent beam laminarity exhibited by the M5838 tube.

Figure 10 illustrates electron trajectories of the scaled gun as predicted by the electron gun program of the Stanford Linear Accelerator Center. The new gun will be evaluated in TMEC's bakable beam analyzer.

TABLE II

COMPARISON OF CIRCUIT DESIGNS A AND B

DESIGN A

FREQUENCY	5GHz	8GHz	10.5 GHz
INPUT CKT I a = .162 cm, b = .278 cm, Pitch = .232 cm			
Phase Velocity	.2113	.2022	.1976
Axial Impedance	35.5	20.5	10.4
γa	.79	1.32	1.77
ka	.17	.27	.36
OUTPUT CKT II a = .173 cm, b = .278 cm, Pitch = .255 cm			
Phase Velocity	.2061	.2022	.1990
Axial Impedance	30.2	15.1	7.0
γa	.86	1.40	1.87
ka	.18	.29	.38
OUTPUT CKT III a = .173 cm, b = .278 cm, Pitch = .245 cm			
Phase Velocity	.1983	.1947	.1916
Axial Impedance	30.7	15.6	6.9
γa	.89	1.46	1.94
ka	.18	.29	.38
OUTPUT CKT IV a = .162 cm, b = .278 cm, Pitch = .228 cm			
Phase Velocity	.2078	.1989	.1944
Axial Impedance	36.3	17.4	7.9
γa	.80	1.34	1.80
ka	.17	.27	.36
OUTPUT CKT V a = .162 cm, b = .278 cm, Pitch = .224 cm			
Phase Velocity	.2039	.1952	.1907
Axial Impedance	37.0	18.0	8.5
γa	.82	1.37	1.84
ka	.17	.27	.36

DESIGN B

FREQUENCY	5GHz	8GHz	10.5GHz
INPUT CKT I a = .174 cm, b = .298 cm, Pitch = .260 cm			
Phase Velocity	.2107	.2062	.2041
Axial Impedance	35.0	14.0	5.8
γa	.84	1.38	1.83
ka	.18	.29	.38
OUTPUT CKT II a = .185 cm, b = .298 cm, Pitch = .287 cm			
Phase Velocity	.2106	.2062	.2016
Axial Impedance	25.1	12.1	4.5
γa	.90	1.47	1.97
ka	.19	.31	.41
OUTPUT CKT III a = .185 cm, b = .298 cm, Pitch = .259 cm			
Phase Velocity	.1926	.1887	.1866
Axial Impedance	26.9	12.4	4.5
γa	.99	1.61	2.14
ka	.19	.31	.41
OUTPUT CKT IV a = .174 cm, b = .298 cm, Pitch = .246 cm			
Phase Velocity	.2036	.1989	.1965
Axial Impedance	38.2	13.8	5.1
γa	.88	1.44	1.91
ka	.18	.29	.38
OUTPUT CKT V a = .174 cm, b = .298 cm, Pitch = .255 cm			
Phase Velocity	.2071	.2027	.2006
Axial Impedance	35.2	14.3	6.1
γa	.86	1.41	1.87
ka	.18	.29	.38

Figure 4. Phase velocity, Design B circuits.

-11-

Output I: a = .0684
            9.79 TPI

Output II: a = .0727
            8.84 TPI

Output III: a = .0727
            9.81 TPI

Output IV: a = .0684
            10.31 TPI

Axial Impedance

Frequency (GHz)
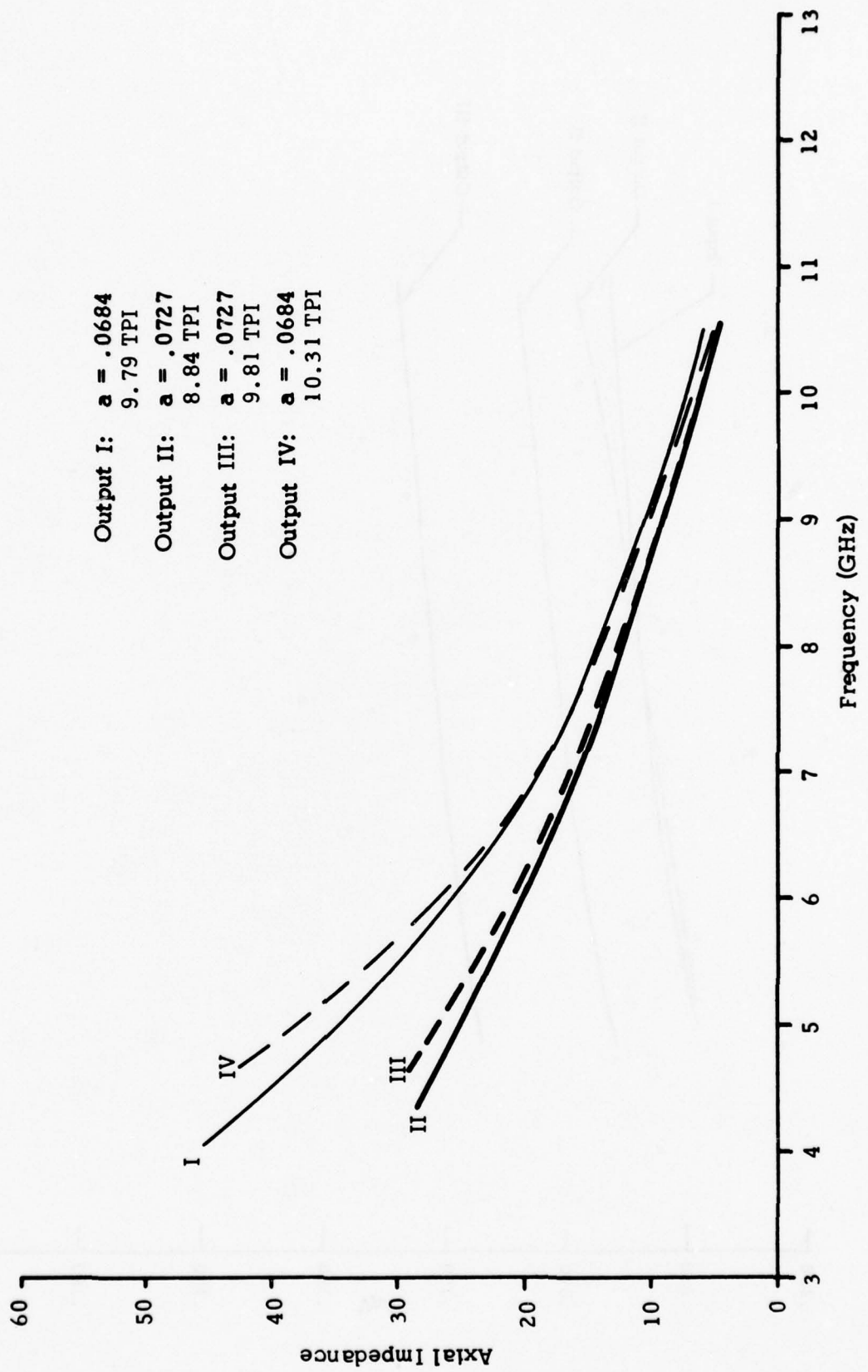
Figure 5. Design B circuits without vanes.
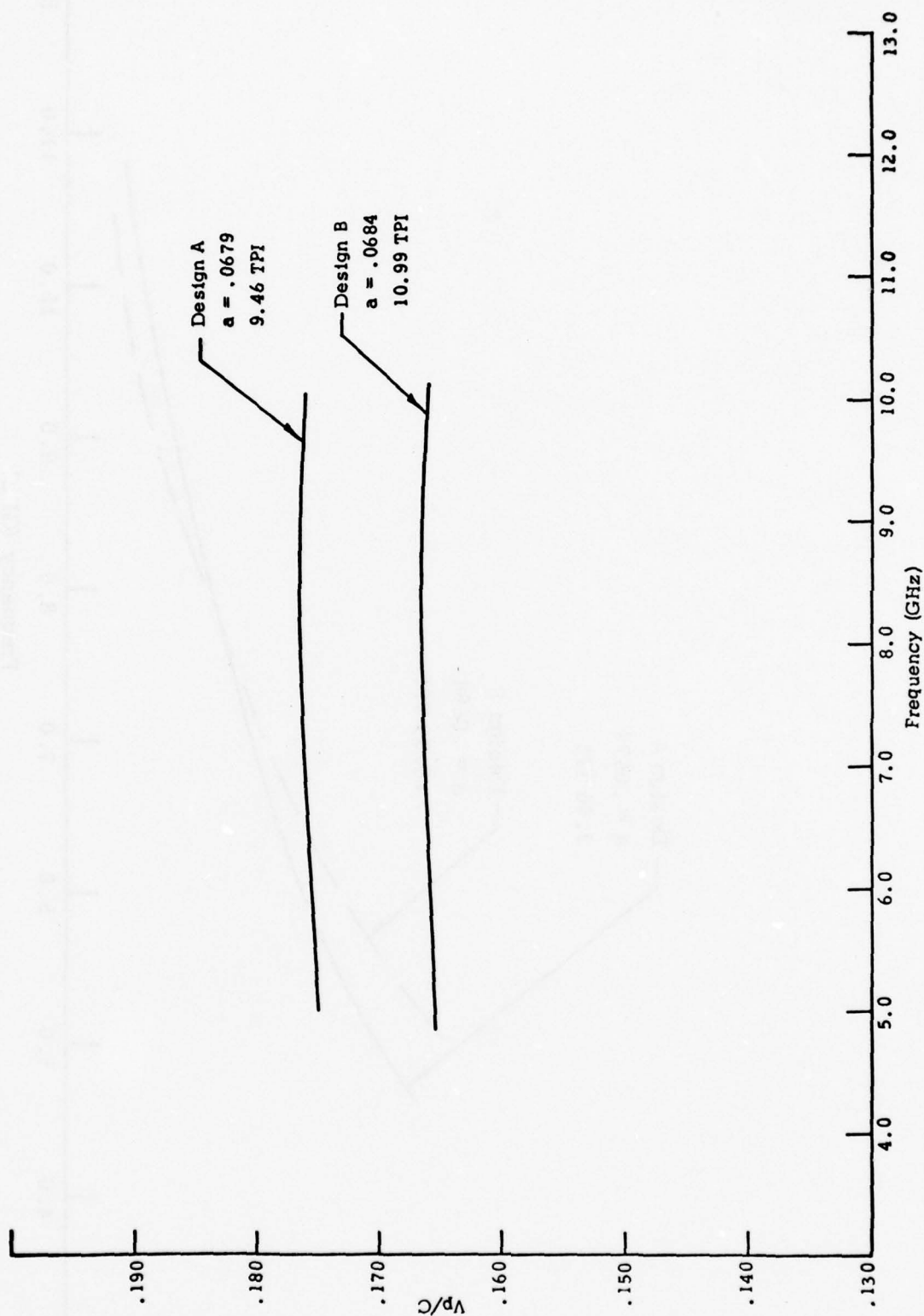
Figure 6. Normalized phase velocity for vane-loaded small-diameter circuits.
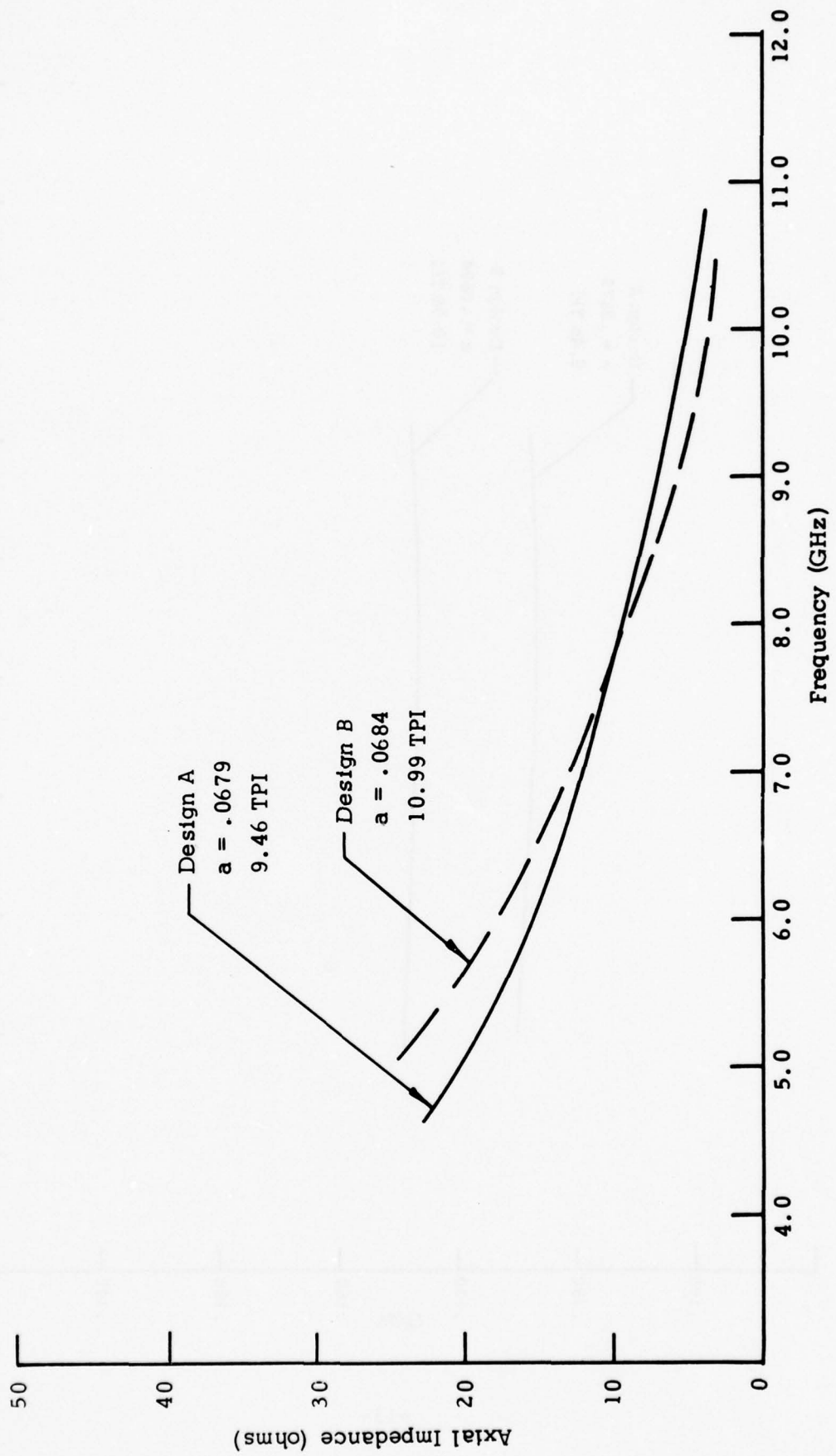
Figure 7. Axial impedance for vane-loaded small-diameter circuits.

Frequency (GHz)

Axial Impedance (ohms)

Design A
a = .0679
9.46 TPI

Design B
a = .0684
10.99 TPI
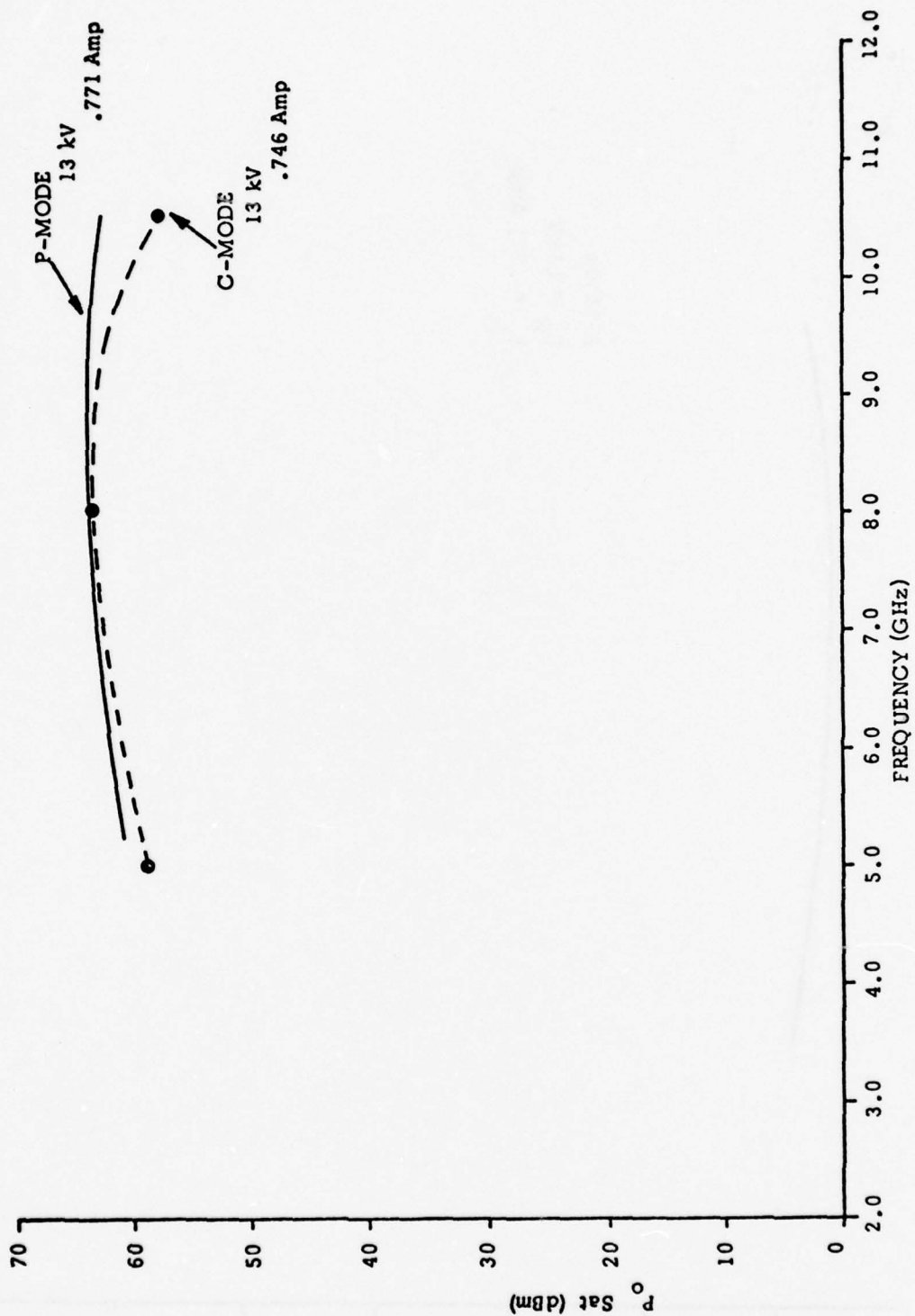
Figure 8. Computer-predicted performance of Model A.
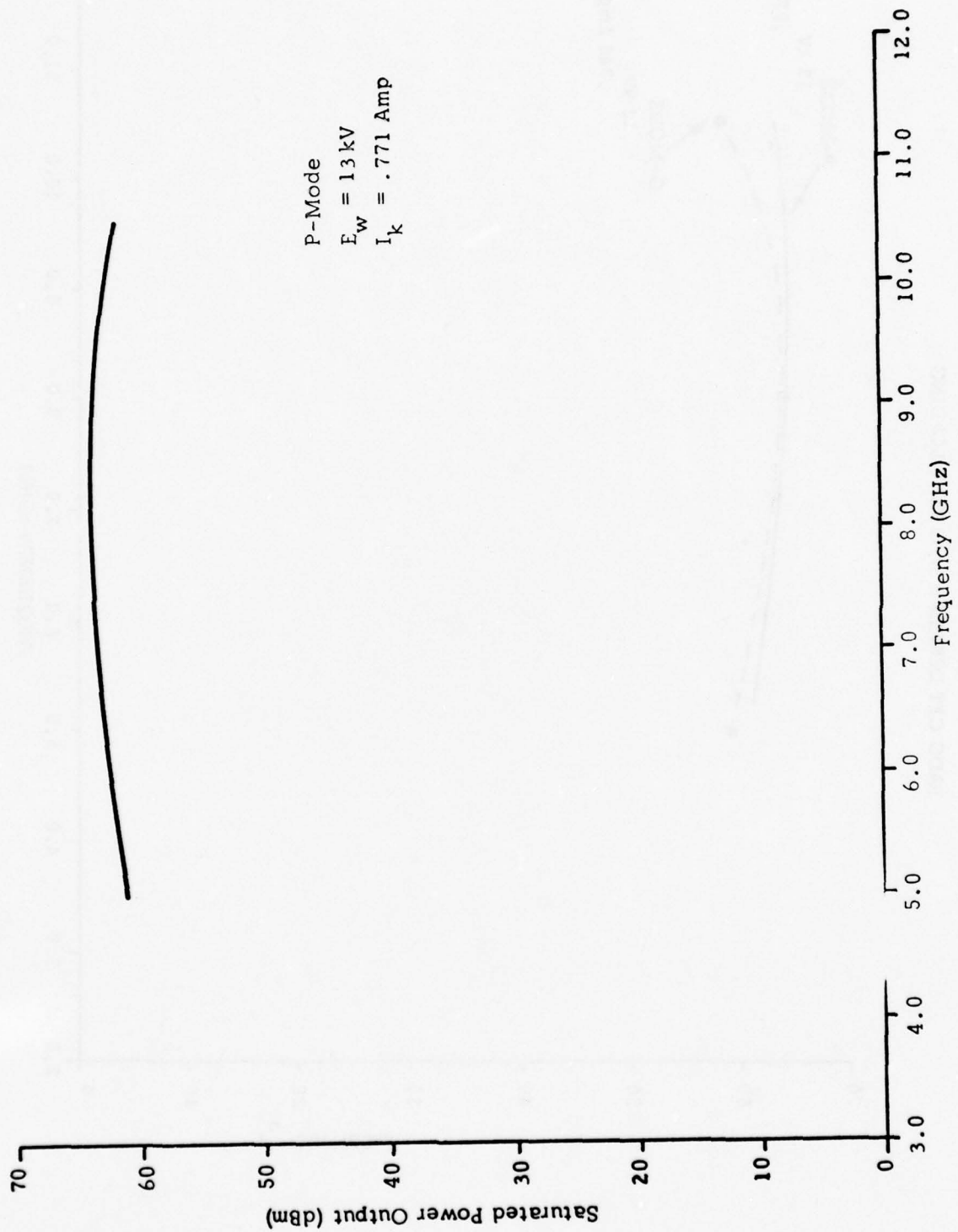
Figure 9. Computer-predicted performance of Model B without vane loading.
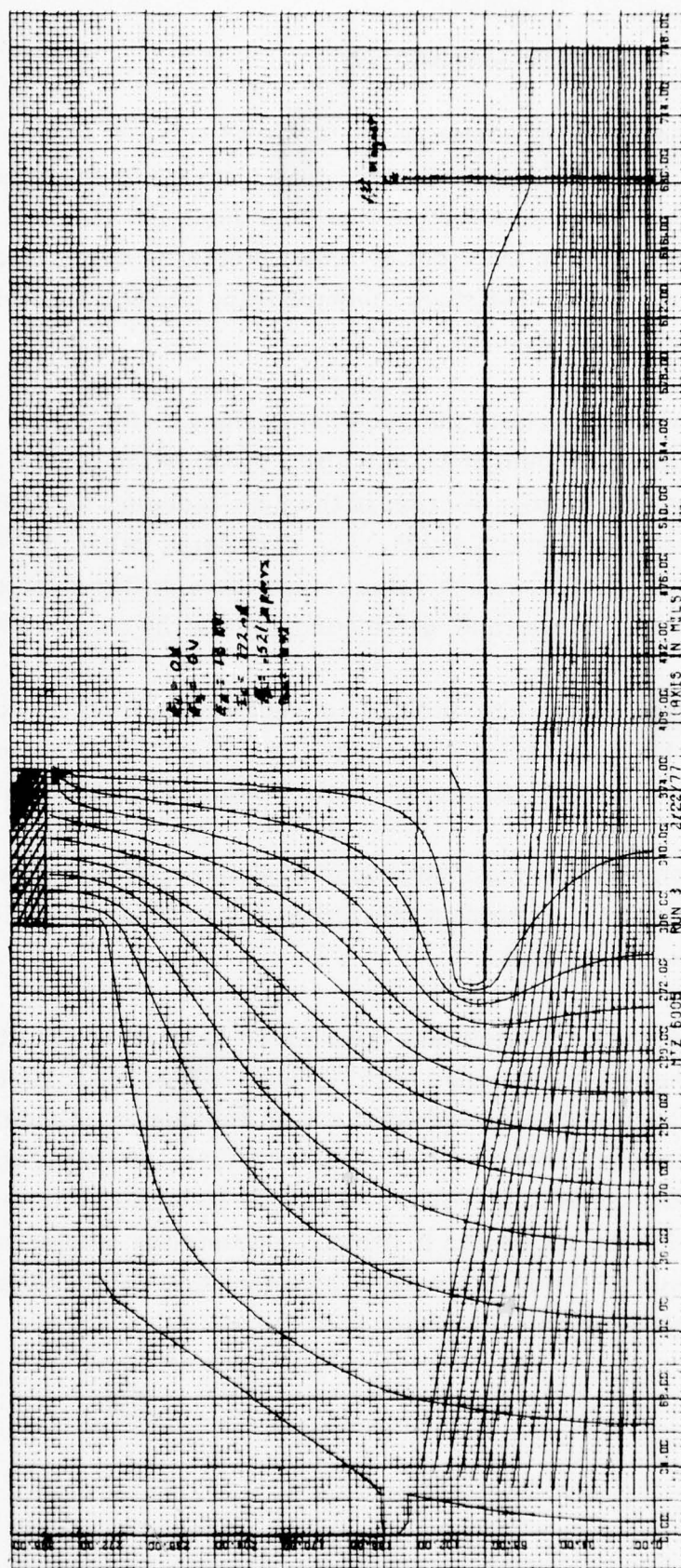
Figure 10. Computer plot of electron trajectories for new gun of Model B.

3.3   PPM Focusing Design

To explain the focusing design of the proposed tube, it is helpful to discuss the focusing of the M5838 tube. This tube employs Alnico 8 magnets and operates with a focusing structure that provides a $\frac{\lambda p}{L}$ of 2.0. For optimum beam stiffness, $\frac{\lambda p}{L}$ on the order of 3.5 or greater is desirable. To obtain this condition, a new PPM stack incorporating samarium cobalt magnets with $\frac{\lambda p}{L} = 4.0$ was designed.

Figures 11 and 12 illustrate the two PPM designs, with Figure 11 showing the design to be used for design A which fits the existing M5838 barrel, and Figure 12 showing a cross section of the Sm-Co design to be used on the design B version of the MTZ-6005. The calculated value of $\frac{\lambda p}{L}$ for both these designs is 4.5, a high enough value to provide a stiffly-focused beam that will be much less prone to RF defocusing than is the current M5838 tube.

The Sm-Co PPM design also provides a much higher field on axis. The design value of the field for design A provides a peak field of 2180 gauss and the design B configuration will provide a magnetic field of 2030 gauss.

Care has been taken in the PPM design to ensure that pole pieces are not driven to saturation. Maximum field expected in these pole pieces will be less than 14,500 oersteds.

Both of these magnetic structures have been designed and built. Figure 13 illustrates the results obtained from the Sm-Co PPM stack for design A. The results illustrate very close agreement with the design calculations, with peak fields ranging between 2100 and 2450 gauss, compared with the design goal of approximately 2200 gauss. Figure 14 illustrates the results obtained from the PPM stack for design B, which demonstrates similar agreement with predicted results. Peak fields range between 1950 and 2300 gauss, with the design objective being 2050 gauss.
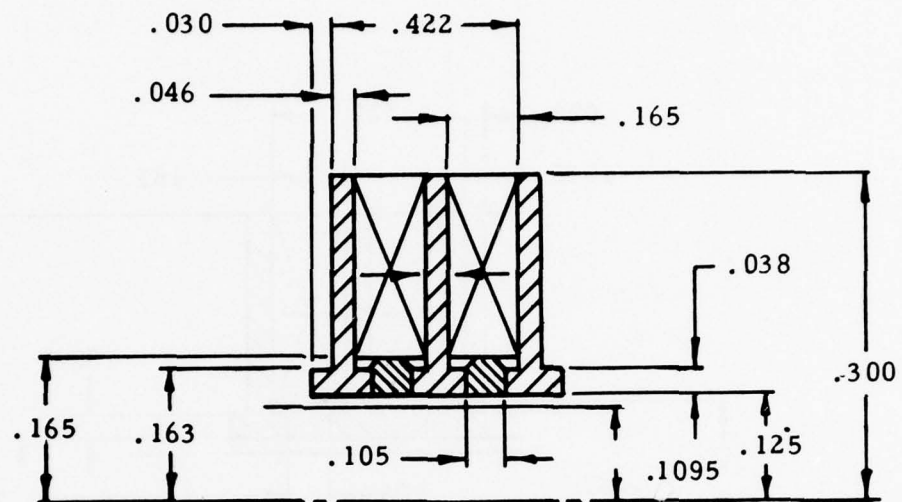
$\underline{SmCo}$

$\hat{B} = 2,188$ Gauss

$\bar{\gamma} = .038$ in.

$\dfrac{\lambda_p}{L} = \dfrac{.036 \times .038}{.422 \sqrt{.52 \times 10^{-6}}} = 4.5$

Maximum Field Within Iron = 14,651 oersteds

Figure 11. Design A for existing barrel.

SmCo

$\hat{B}$ = 2,032 Gauss

$\overline{\gamma}$ = .038 In

$\dfrac{\lambda P}{L}$ = $\dfrac{.036 \times .038}{.422\diagup.52 \times 10^{-6}}$ = 4.5

MAX FIELD WITHIN IRON = 14,140 OER.

Figure 12. Design B for new barrel.
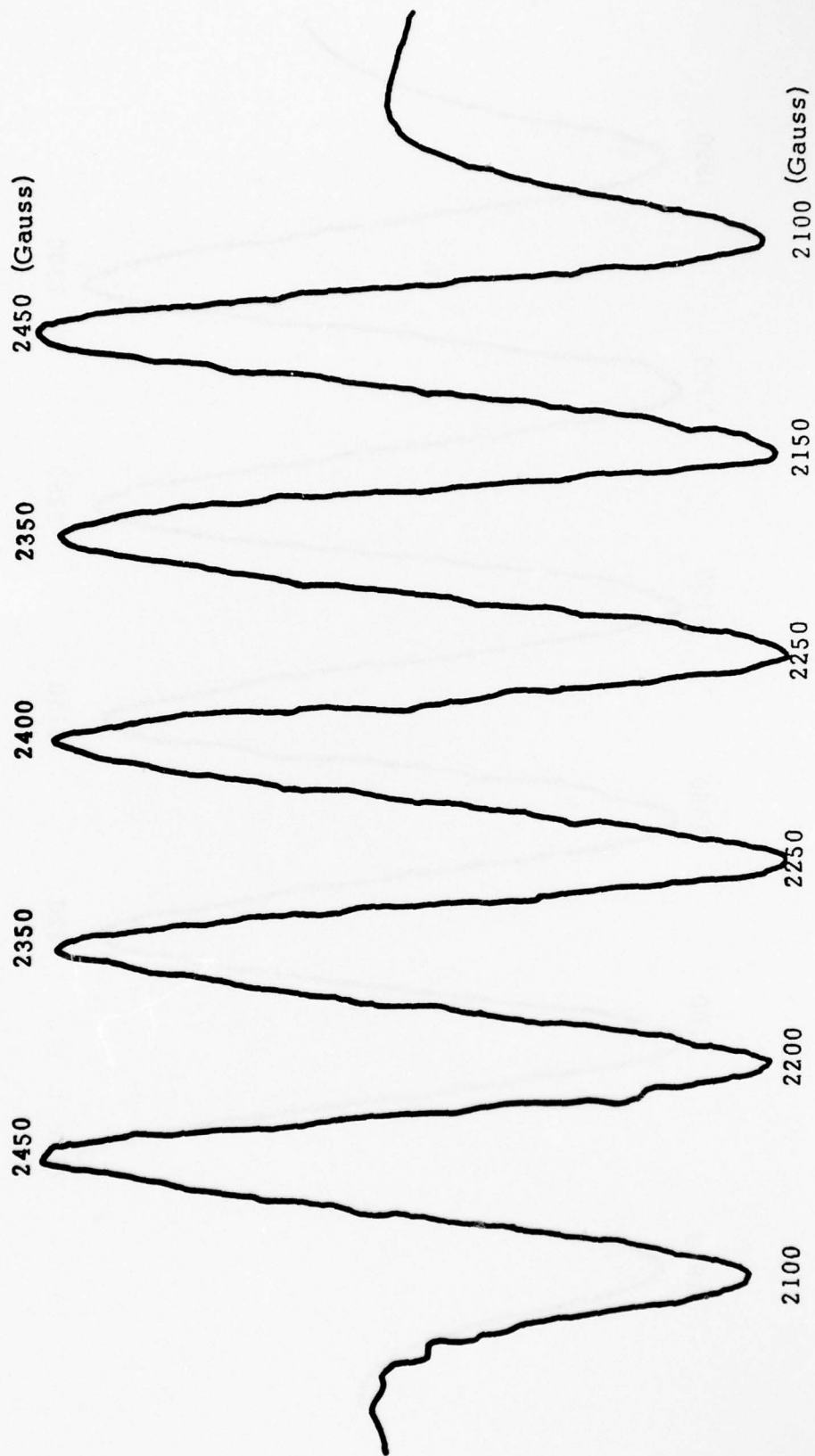
Figure 13. PPM stack profile, design A.
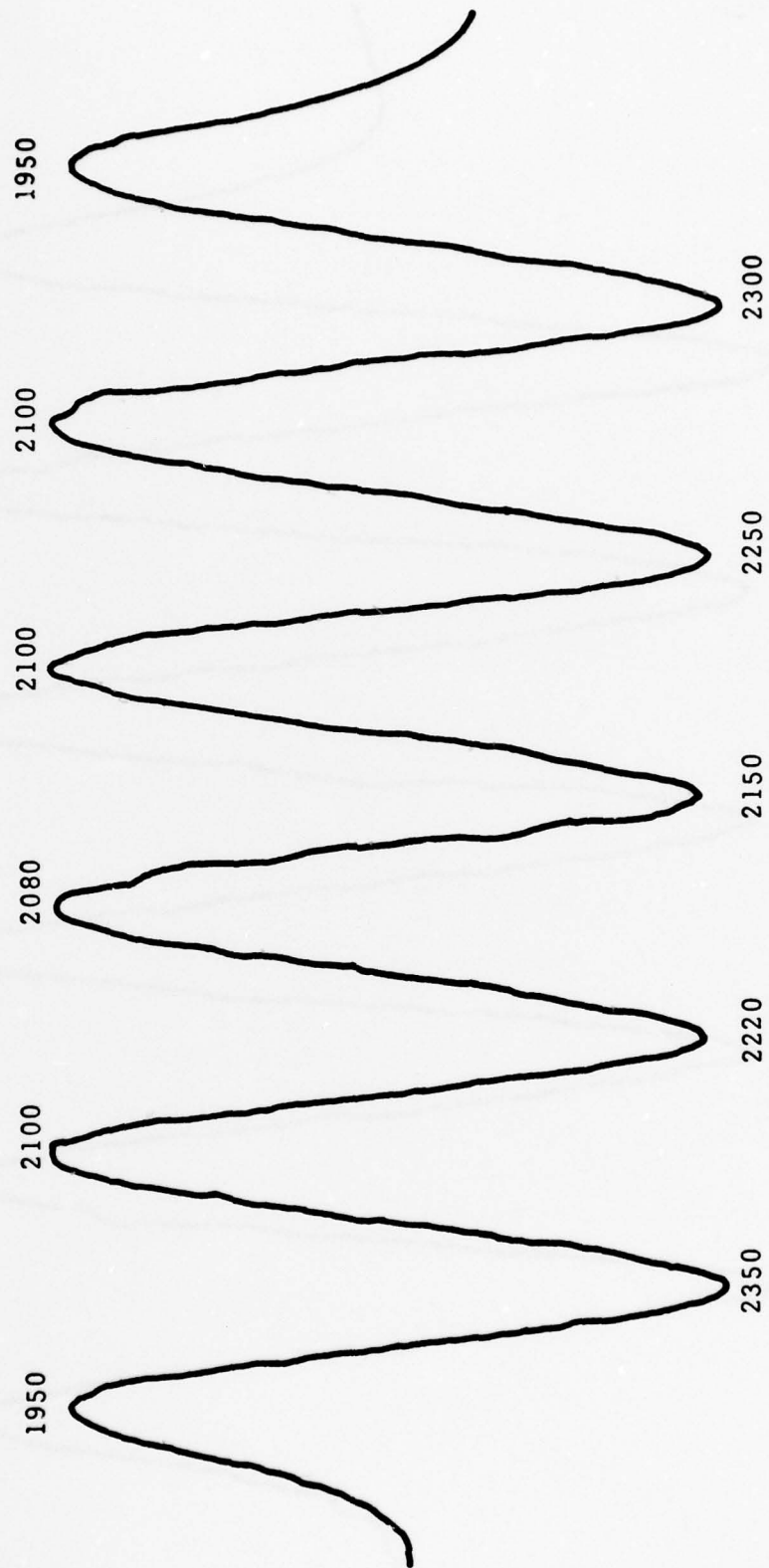
Figure 14. PPM stack profile, design B.

3.4 Waveguide Transition

Considerable time has been devoted to design of the output impedance transition for the new tube. The design used on similar existing high-band dual mode tubes consists of a helix connected to a coaxial transmission line that runs through a ceramic window to another coaxial transmission line leading to a double-ridged waveguide. The impedance match is attained by adjustment of a sliding short on the waveguide and by several tuning elements that are placed in the waveguide.

It is difficult to achieve an impedance match of less than 2:1 VSWR with this existing design. For high power applications, it offers poor RF breakdown resistance since it requires the introduction of relatively high mismatches to cancel out other existing mismatches. The ceramic window is made of aluminum oxide and has a relatively low characteristic impedance of about 40 ohms; even with broadband design techniques, it is hard to make this window transparent to impedances higher than 55 ohms. This results in a relatively high built-in mismatch between the window and other elements.

The final match element is the waveguide. The double-ridge waveguide has an effective characteristic impedance varying from approximately 325 ohms at the low end of the band to about 250 ohms at the high end of the band. In the present configuration, steps are used in the waveguide to reduce the impedance, but they are not properly designed to minimize the VSWR of the step transitions.

In summary, then, the problem was that there were three elements in this transition that had incompatible characteristic impedances. The new design attempted to bring all of these individual components closer to the same characteristic impedance to minimize the effect of the transformers, adjustment screws and tuning elements on the match.

The first step in the new design was to change the ceramic window material from aluminum oxide to beryllium oxide, thereby realizing a substantial increase in the characteristic impedance of the window itself as a result of the lower dielectric constant of beryllia (6) compared to the dielectric constant of aluminum oxide (9).

The objective in designing this new window was to obtain the highest possible impedance, which usually involves having a relatively high ratio of outer conductor OD to center conductor ID. However, increasing the size of the OD is limited by introduction of higher order modes in the coaxial line, and reducing the ID of the center conductor is limited by mechanical and thermal considerations.

In arriving at a compromise design suitable to the proposed tube, TMEC utilized COMPACT, a microwave circuit optimization computer program to achieve a new beryllia oxide window design that is transparent to 73 ohms over the band and will not propagate higher order modes until 12 GHz. Test results for the window are shown in Figure 15, which plots the VSWR looking through the window versus system impedance for three frequencies. For all three frequencies, the window is highly transparent at 73 ohms and has a relatively small VSWR. With respect to 73 ohms, the VSWR is less than 1.1.

Another approach to improvement of the transition has been to reduce the double-ridge waveguide impedance from its high value of approximately 300 ohms to a value of about 90 ohms through the use of a Chebishev transformer. The character of this transformer is that it will provide the minimum VSWR possible for a given length over a given frequency band. Six steps are being used in this transition. The maximum computed VSWR this will yield in transforming the impedance from 300 to 90 ohms will be 1.05 over the band.

Results to date have indicated that these two element redesigns will make possible an impedance match that calls for only a minimum of tuning since

-24-
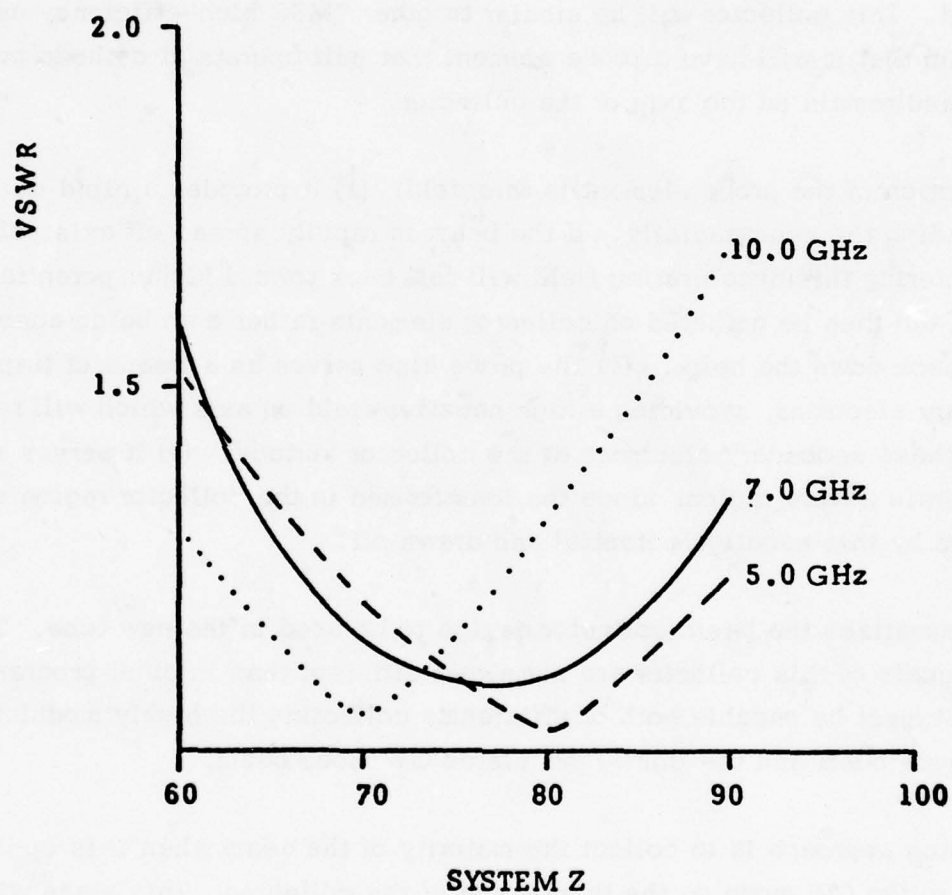
Figure 15. Computer-predicted VSWR for new BeO window.

-25-

the impedances are relatively close; the helix has an impedance of about 75 ohms, the window is transparent to 73 ohms, and the waveguide has an essentially characteristic impedance of 90 ohms.

3.5   Collector Design

The multi-stage collector design is the most important element in the success of this program. The approach taken is to use a three-stage depressed collector utilizing an electrostatically-focused collector that is magnetically shielded. This collector will be similar to other TMEC high-efficiency collectors in that it will have a probe element that will operate at cathode potential and remain on the axis of the collector.

The function of the probe element is threefold: (1) It provides a rapid means of spreading the beam radially. If the beam is rapidly spread off axis, electrons entering this decelerating field will fall back toward higher potential regions and then be gathered on collector elements rather than being accelerated back down the helix. (2) The probe also serves as a means of trapping secondary electrons, providing a high negative field on axis which will repel or trap these secondary electrons at the collector surface. (3) It serves as an ion drain in this region, since the ions formed in the collector region are attracted by this negative potential and drawn off.

This summarizes the basic collector design to be used in the new tube. The design goals of this collector are somewhat different than in other programs in that it must be capable both of efficiently collecting the highly modulated pulse mode beam and the lightly modulated CW mode beam.

The design approach is to collect the majority of the beam when it is operating in the CW mode on the third stage of the collector. This stage will run greatly depressed; in fact, it is planned that this will run at about 15% of cathode potential. Relatively little current will be collected on the first and second stages, which will operate at much higher potentials.

-26-

With this design, when the tube is operated in the pulse mode the beam current will be higher by at least a factor of 2, and the tube will be operating in a saturated condition. Therefore, the velocity spread conditions in the pulse mode will be very severe. Under these conditions, the performance of the collector will be quite different. Since the velocity spread is great and a large number of the electrons have been slowed down, the majority of the beam will be captured on the first and second stages, which run at a much higher potential than the third stage.

As indicated earlier in the design goals chart, the desired collector efficiency in the pulse mode is only required to be on the order of 56%. As a result, the majority of the design effort will be concentrated on obtaining the proper current distribution for the CW mode application, in which collector efficiency must be on the order of 83%.

Computer analysis will depend greatly on the model of the spent beam. The best way of obtaining an accurate spent beam model is to test a similar tube with a multi-stage collector, observing and recording the current distribution of the various stages and for various collector voltages and various RF drive levels. The particular tube that will be used for this has been designed and built and the results will be reported on in the next section.

Computer plots have been run of the initial conditions and are shown in Figures 16, 17 and 18. The key factor in these computer plots is the entrance angle of the electrons into the collector region, which will be correlated with results from the experimental collector. For tubes of this frequency, perveance, power level and focusing structure, there is a range of entrance angles that electrons entering the collector can have, but the range is from $-5°$ to $+5°$. What must be determined experimentally is the weighting factor that will be used for each angle. For example, we can conclude that the majority of electrons will be traveling at the $0°$ angle when they enter the collector, but a very small number of electrons will be entering at $-5°$ and a correspondingly small number at $+5°$. By assigning a weighting factor to the number of electrons at various angles, one can obtain the proper current distribution at each of the stages. What are shown in these three illustrations

Figure 16. Computer plot of current distribution in three-stage collector with probe. Positive angle injection case.

STAGE # 3
E_{b_3} = 2500 VOLTS

STAGE # 2
E_{b_2} = 4320 VOLTS

STAGE # 1
E_{b_1} = 5280 VOLTS

HELIX : E_w = 9660 VOLTS

E_{b_4} = 0

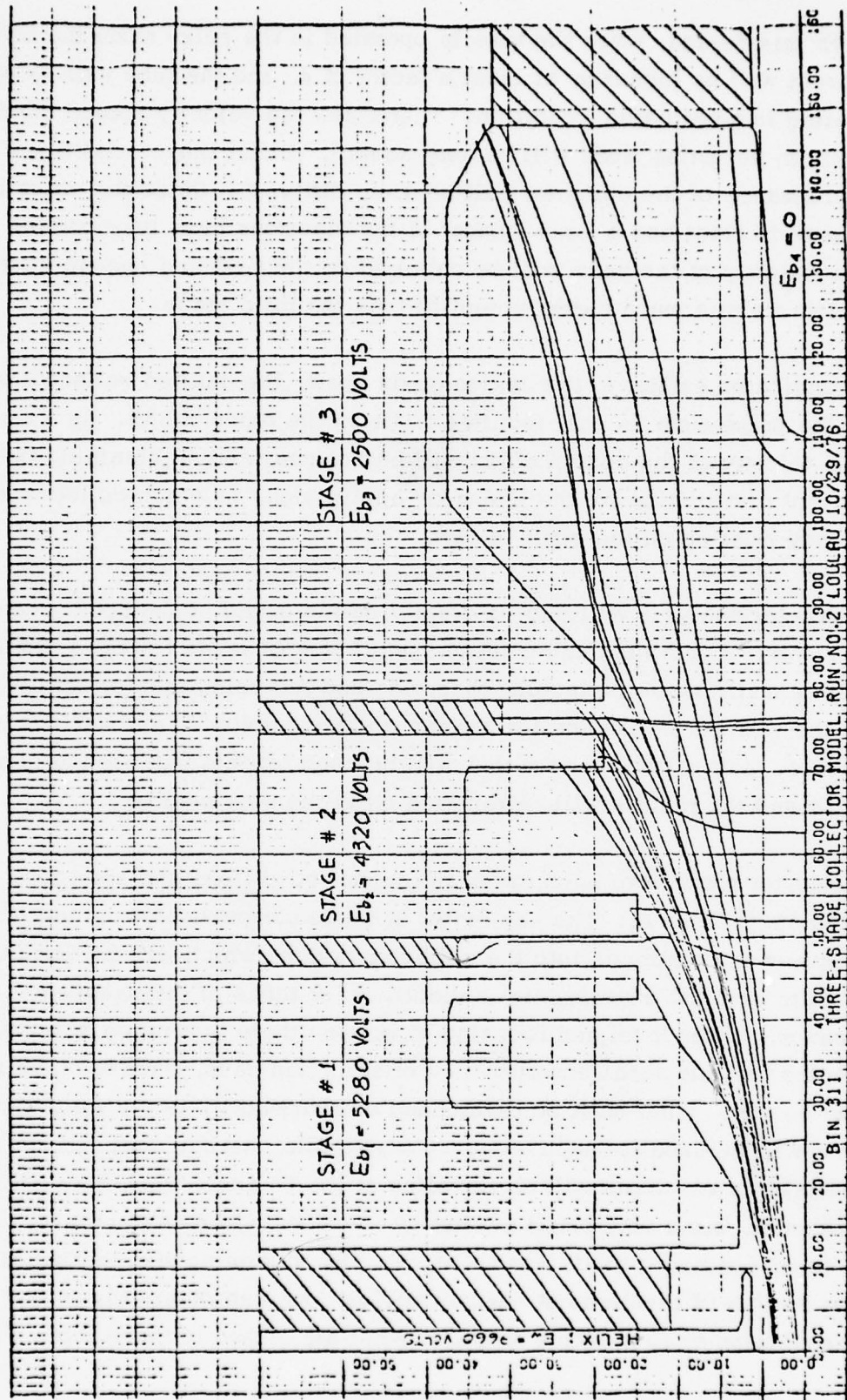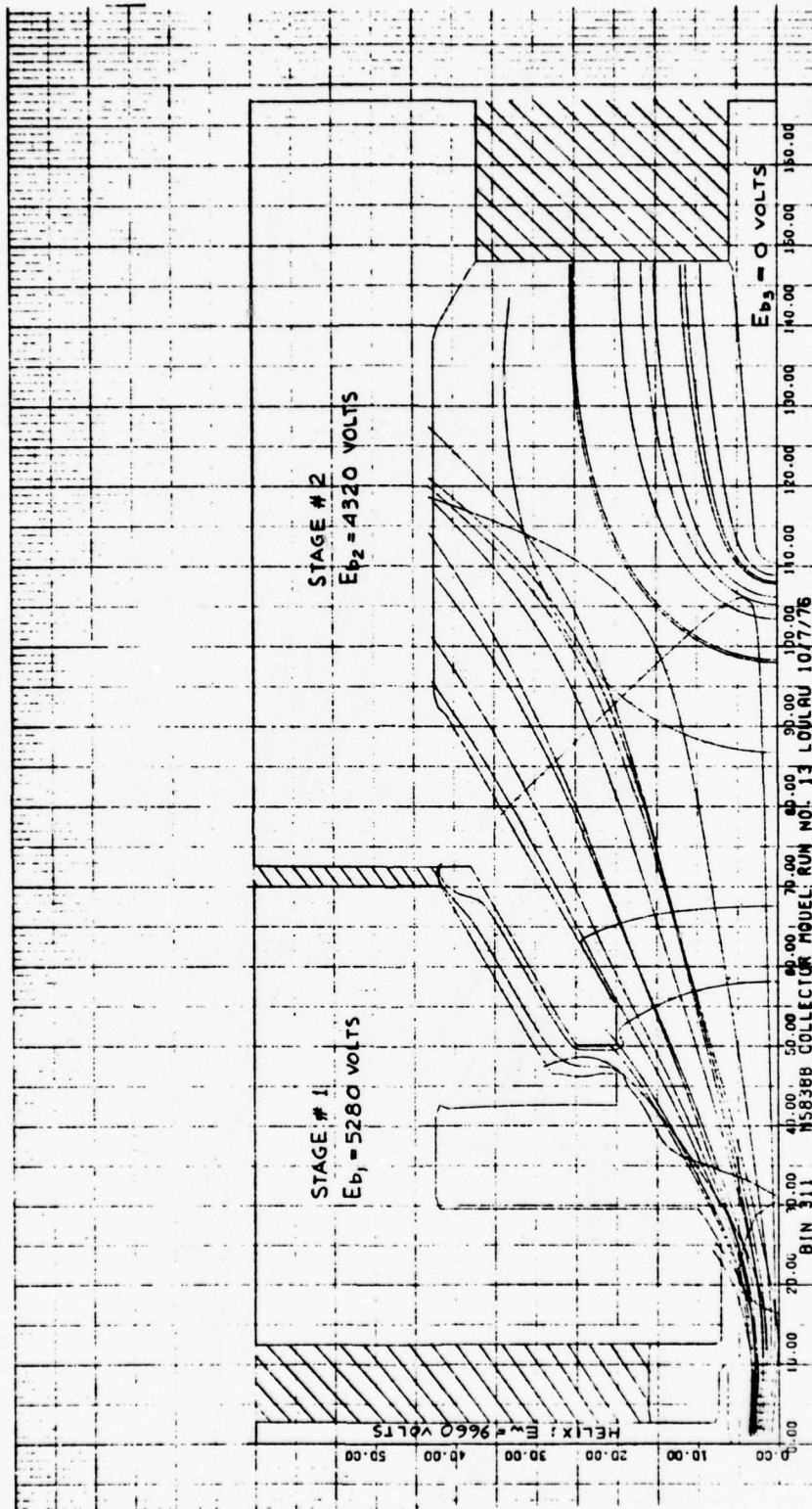THREE-STAGE COLLECTOR MODEL RUN NO.2 LOULAU 10/29/76

BIN 311

Figure 17. Computer plot of current distribution in two-stage collector with probe. Negative angle injection case.
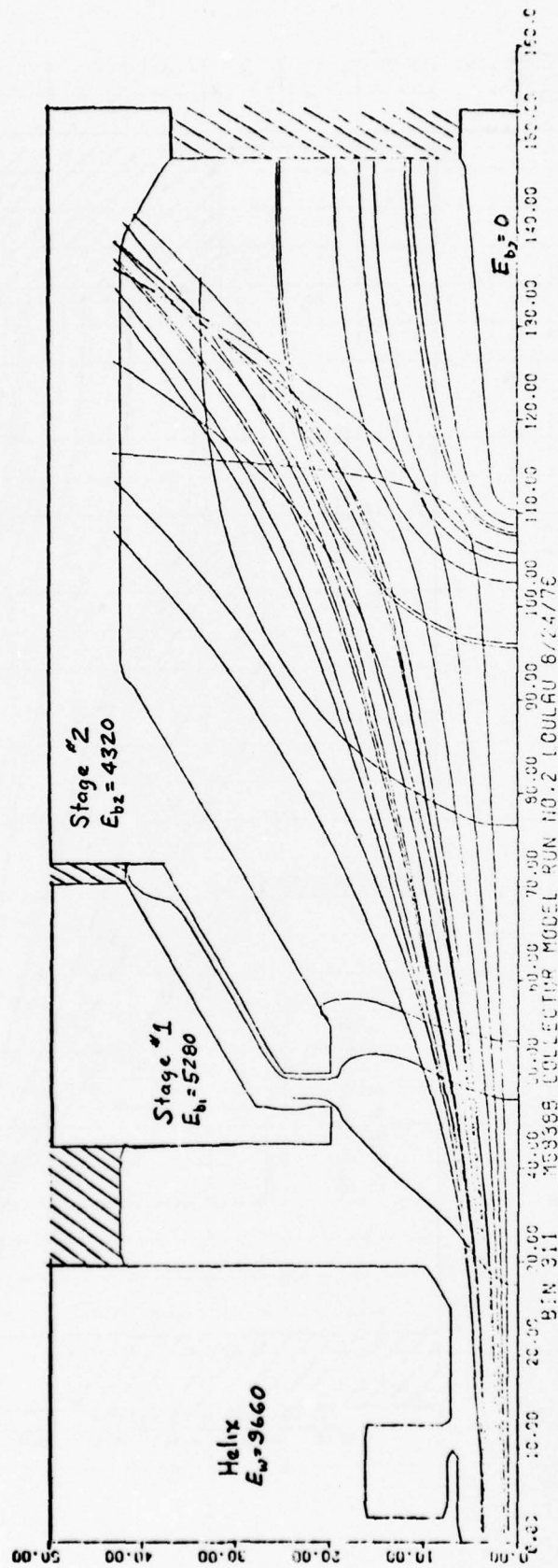
Figure 18. Computer plot of current distribution in two-stage collector with probe. Zero angle injection case.

-30-

are the extremes of the conditions that we have estimated at angles of −5°, 0° and +5°. When experimental results are available, we will put in the correct weighting functions in order to get more accurate results from this study.

The first collector has now been designed. It is very similar to a multi-stage collector used on another program sponsored by the Air Force. Figure 19 shows a cross section of this three-stage, four-element collector with an adjustable probe.

The adjustable probe is used to provide additional freedom in the design, since it is an added way of compensating for imperfect computer modeling.

4.0   TUBE CONSTRUCTION AND TESTING

The first vacuum envelope, VE No. 1, has been built and partially tested. Figure 20 is a photograph of the tube. The focusing obtained with the first vacuum envelope was exceedingly good. Figure 21 illustrates helix and body current as a function of cathode current versus helix voltage.

A great deal of difficulty was encountered in trying to test this tube. The cutoff voltage of the gun was much higher than had been anticipated. A cutoff characteristic of the tube at 13 kV is shown in Figure 22. As indicated in this figure, a focus electrode voltage of 2150 volts was required to obtain proper cutoff conditions. This caused a problem in the testing of the tube in that available modulators have a maximum focus electrode voltage of only 2100 volts. An effort is currently under way to modify an existing modulator to allow a higher cutoff voltage. It is expected that modification of the focus electrode to cathode spacing will reduce the voltage required to obtain cutoff.

Despite this problem, VE No. 1 has undergone preliminary RF testing by using a cathode modulator. Unfortunately, the cathode modulator is limited to a duty factor of .1% and independent collector supplies are not available. As a result, we were unable to obtain meaningful data about the collector characteristics.

Figure 19. Experimental three-stage collector.

12-2191
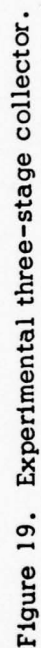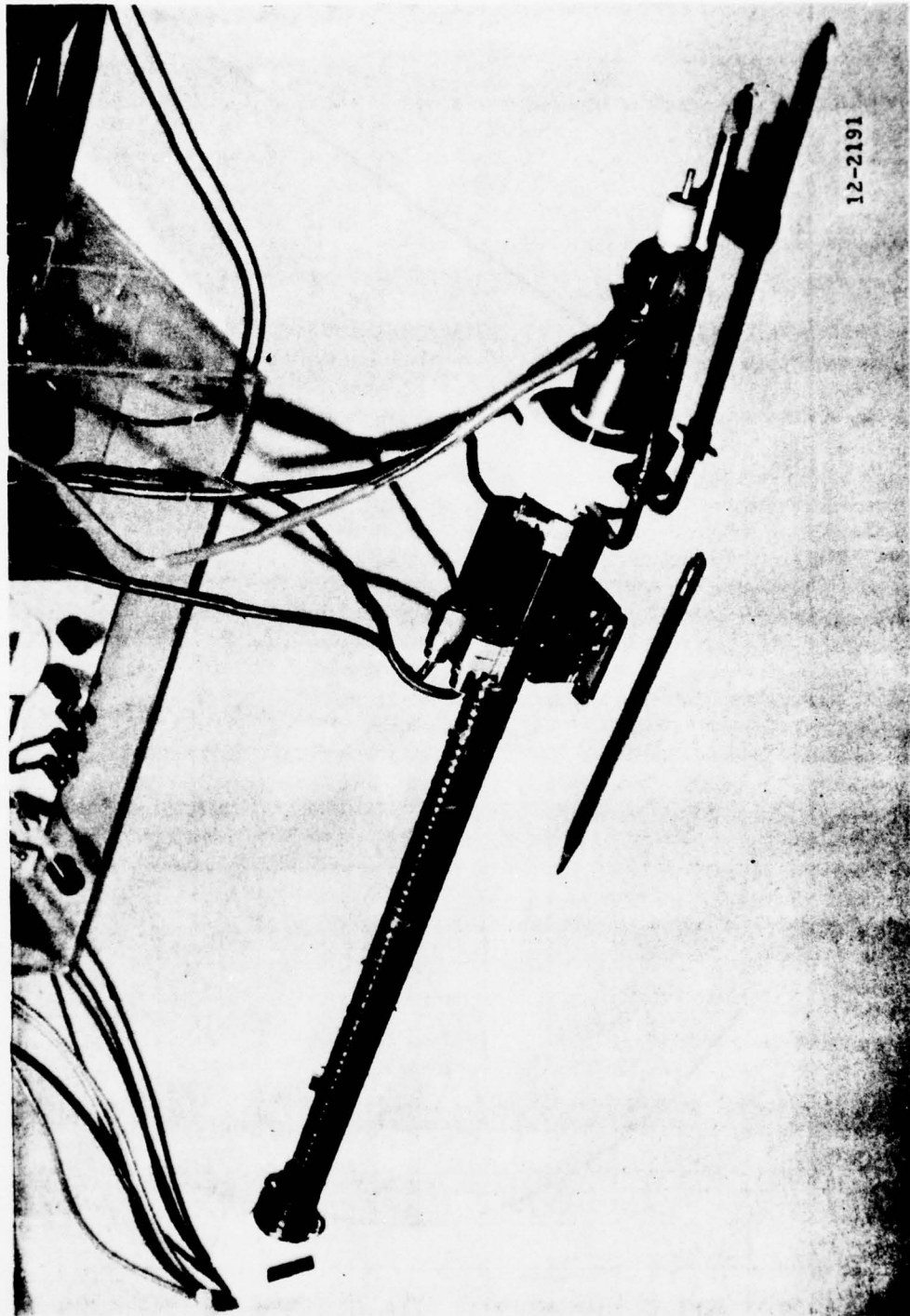
Figure 20. First experimental tube of design A.

-33-
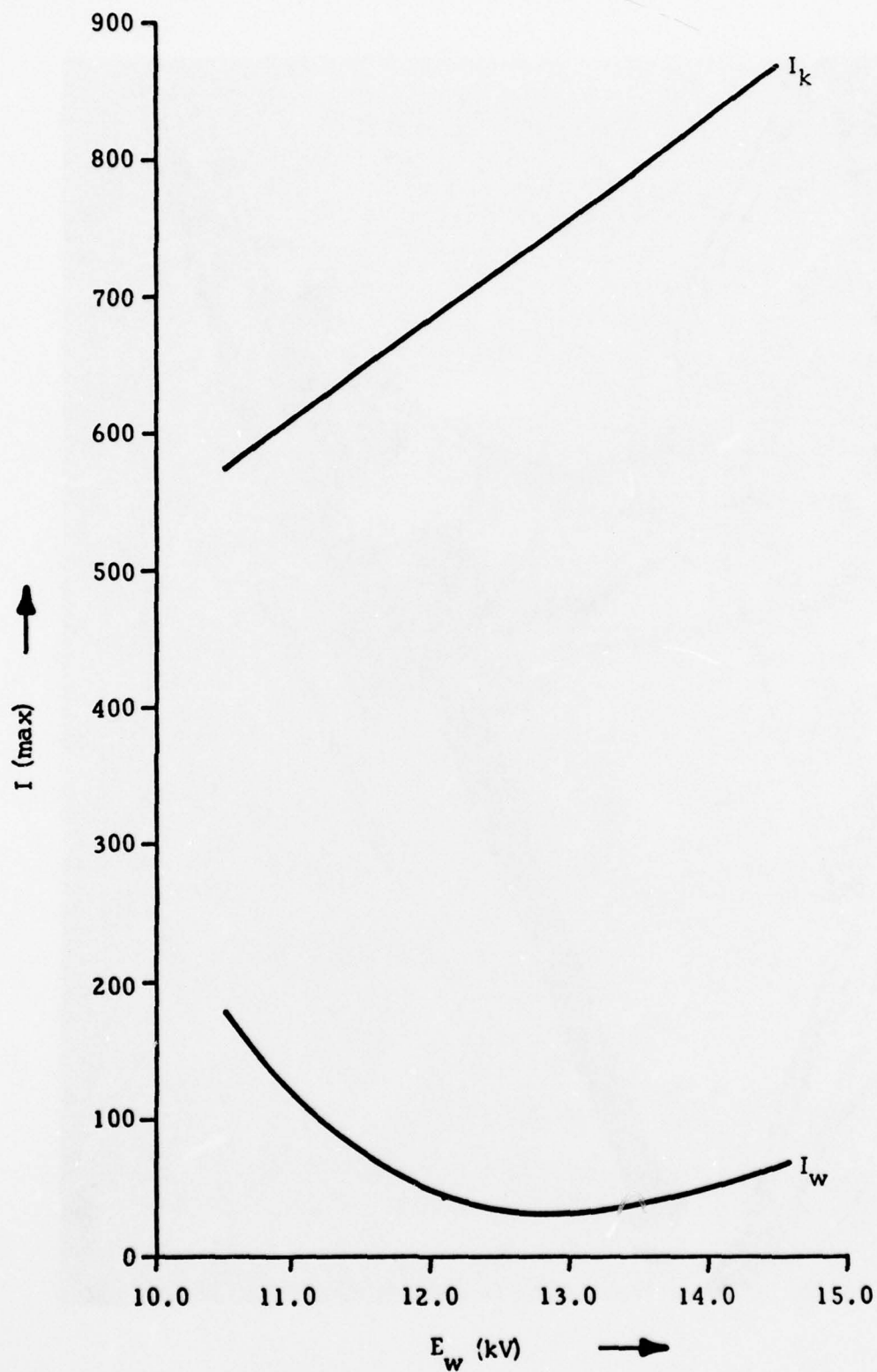
Figure 21. Helix and cathode currents versus helix voltages
for tube SN 1.
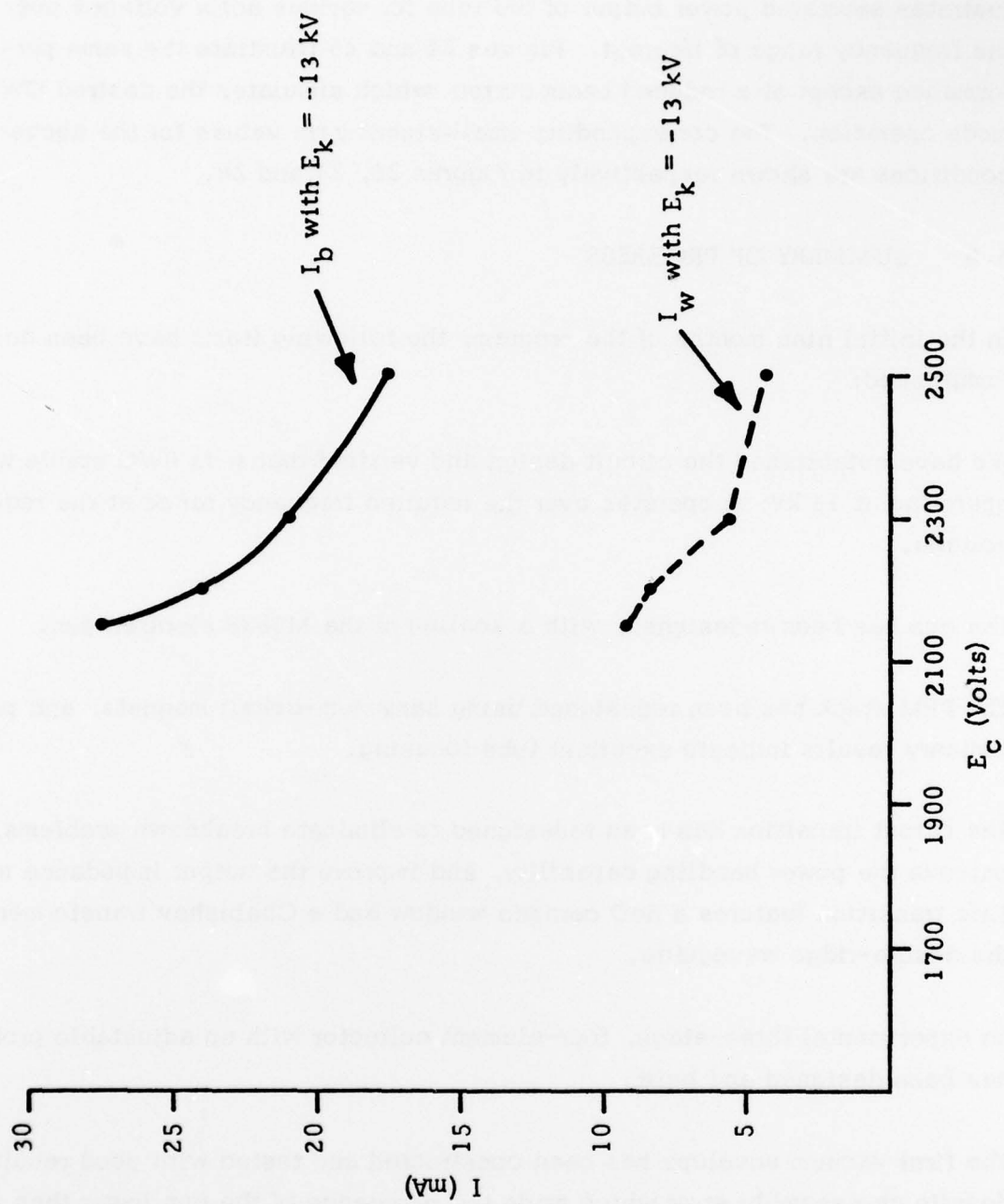
Figure 22. Cutoff characteristic of tube SN 1.

The preliminary RF data is very encouraging, however, as it illustrates that the tube is BWO stable and very well centered in frequency. Figure 23 illustrates saturated power output of the tube for various helix voltages over the frequency range of interest. Figures 24 and 25 illustrate the same performance except at a reduced beam current which simulates the desired CW mode operation. The corresponding small-signal gain values for the above conditions are shown respectively in Figures 26, 27 and 28.

5.0 SUMMARY OF PROGRESS

In the initial nine months of the program, the following items have been accomplished:

We have established the circuit design and verified that it is BWO stable while operating at 13 kV; it operates over the required frequency range at the required voltage.

The gun has been redesigned, with a scaling of the M5838 electron gun.

The PPM stack has been redesigned using samarium-cobalt magnets, and preliminary results indicate excellent tube focusing.

The output transition has been redesigned to eliminate breakdown problems, improve the power handling capability, and improve the output impedance match. This transition features a BeO ceramic window and a Chebishev transformer in the double-ridge waveguide.

An experimental three-stage, four-element collector with an adjustable probe has been designed and built.

The first vacuum envelope has been constructed and tested with good results despite an assembly error which made the perveance of the gun lower than anticipated. Despite this error, the tube was operated at the proper design voltage and demonstrated encouraging performance.
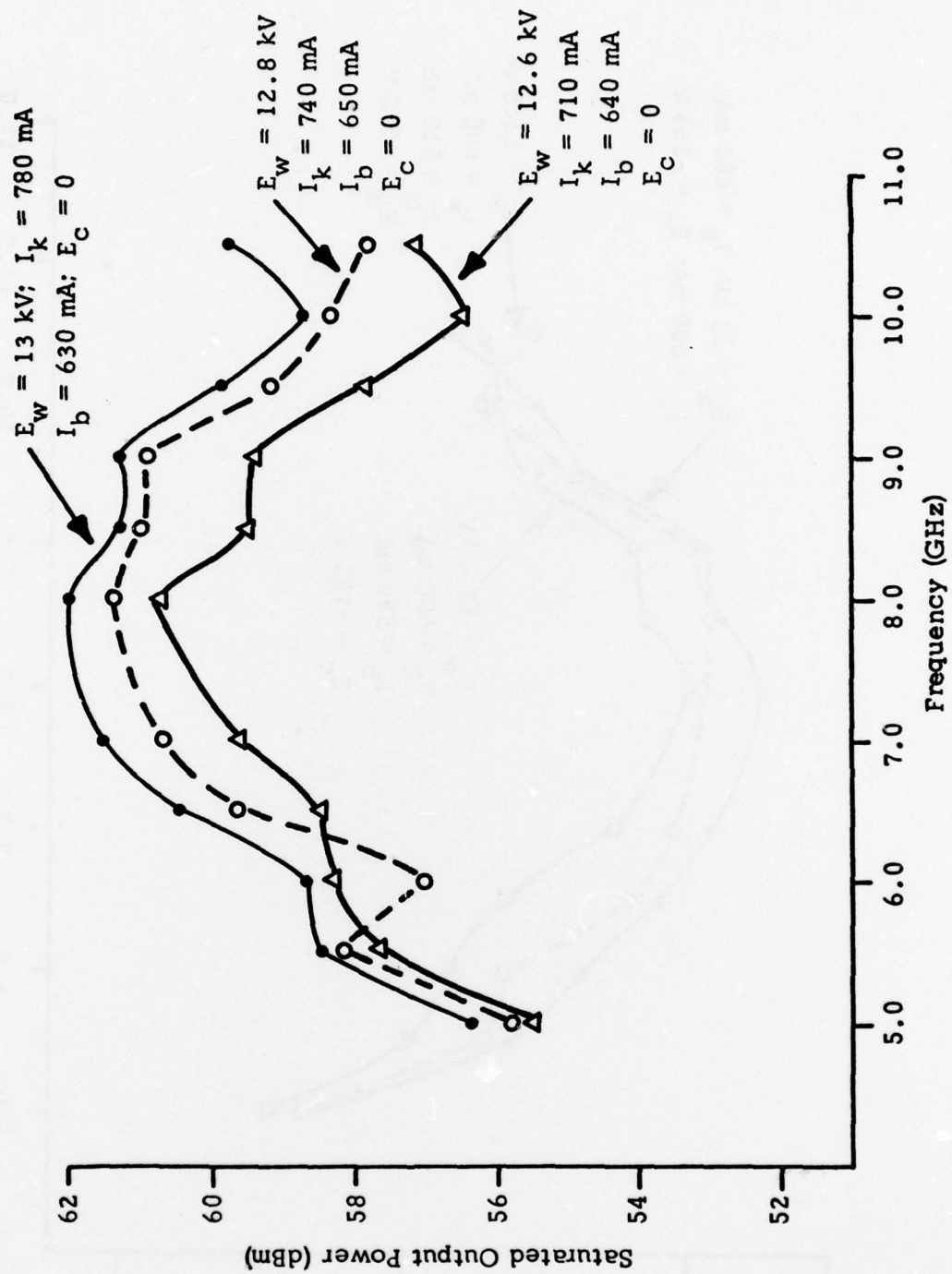
Figure 23. Saturated output power for various helix voltages of tube SN 1.

$E_w = 13$ kV; $I_k = 600$ mA
$I_b = 500$ mA; $E_c = -165$ V

$E_w = 12.8$ kV
$I_k = 600$ mA
$I_b = 510$ mA
$E_c = -135$ V

$E_w = 12.6$ kV
$I_k = 600$ mA
$I_b = 590$ mA
$E_c = -105$ V

Frequency (GHz)

Saturated Output Power (dBm)
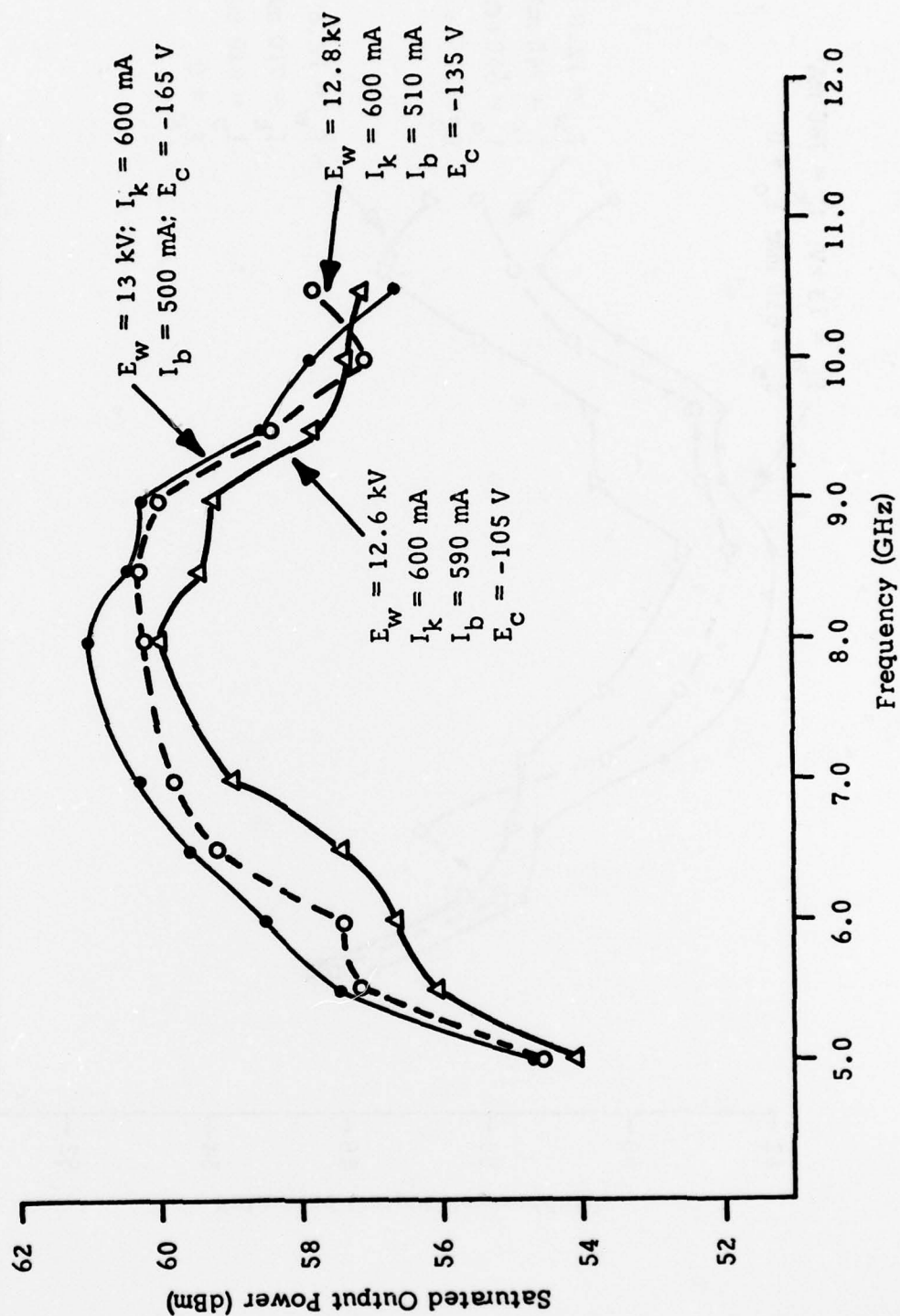
Figure 24. Saturated output power at reduced beam currents for various helix voltages of tube SN 1.
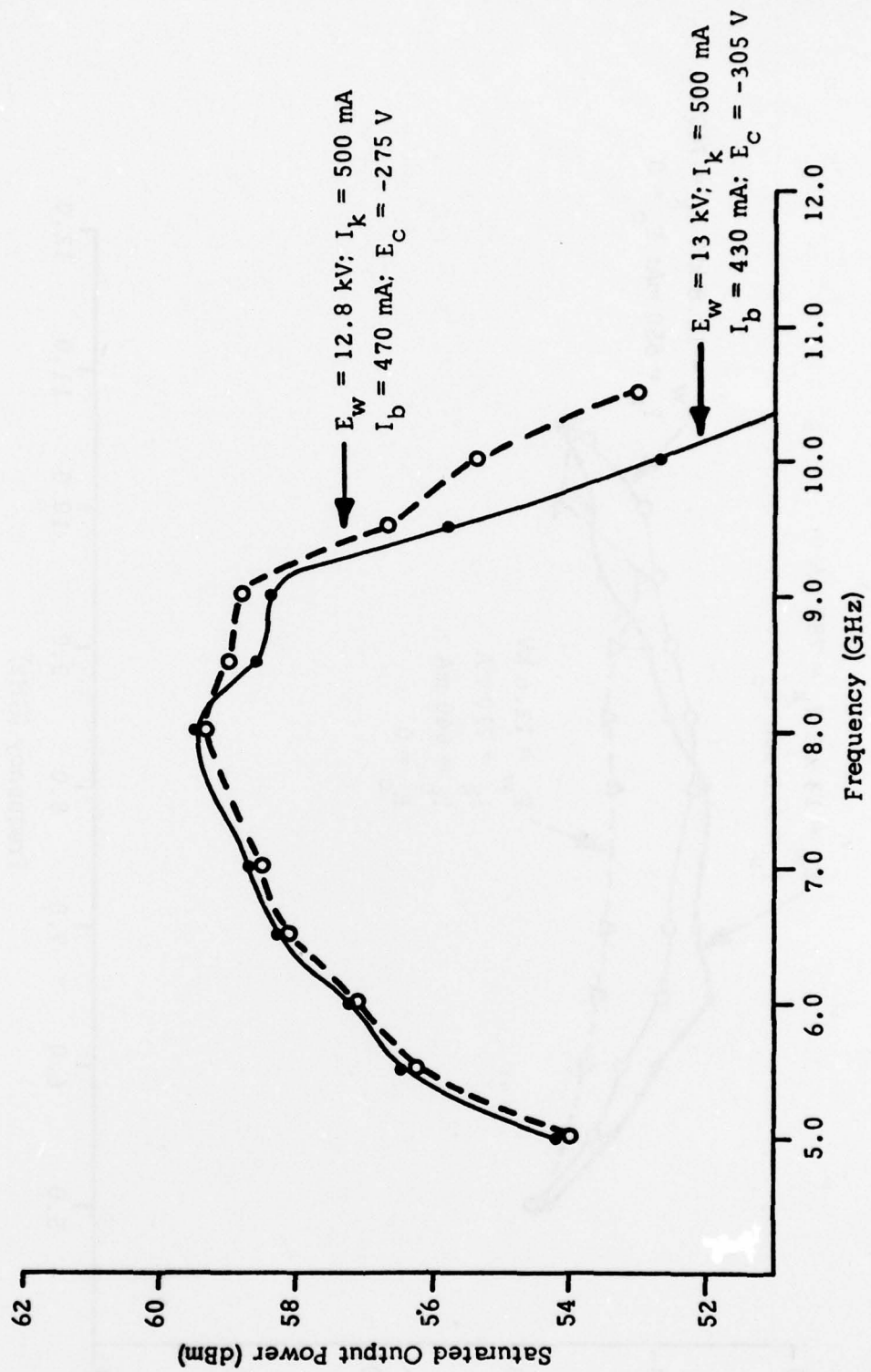
Figure 25. Saturated output power at reduced beam currents for various voltages of tube SN 1.

$E_w = 12.8$ kV; $I_k = 500$ mA
$I_b = 470$ mA; $E_c = -275$ V

$E_w = 13$ kV; $I_k = 500$ mA
$I_b = 430$ mA; $E_c = -305$ V

Frequency (GHz)

Saturated Output Power (dBm)

-39-
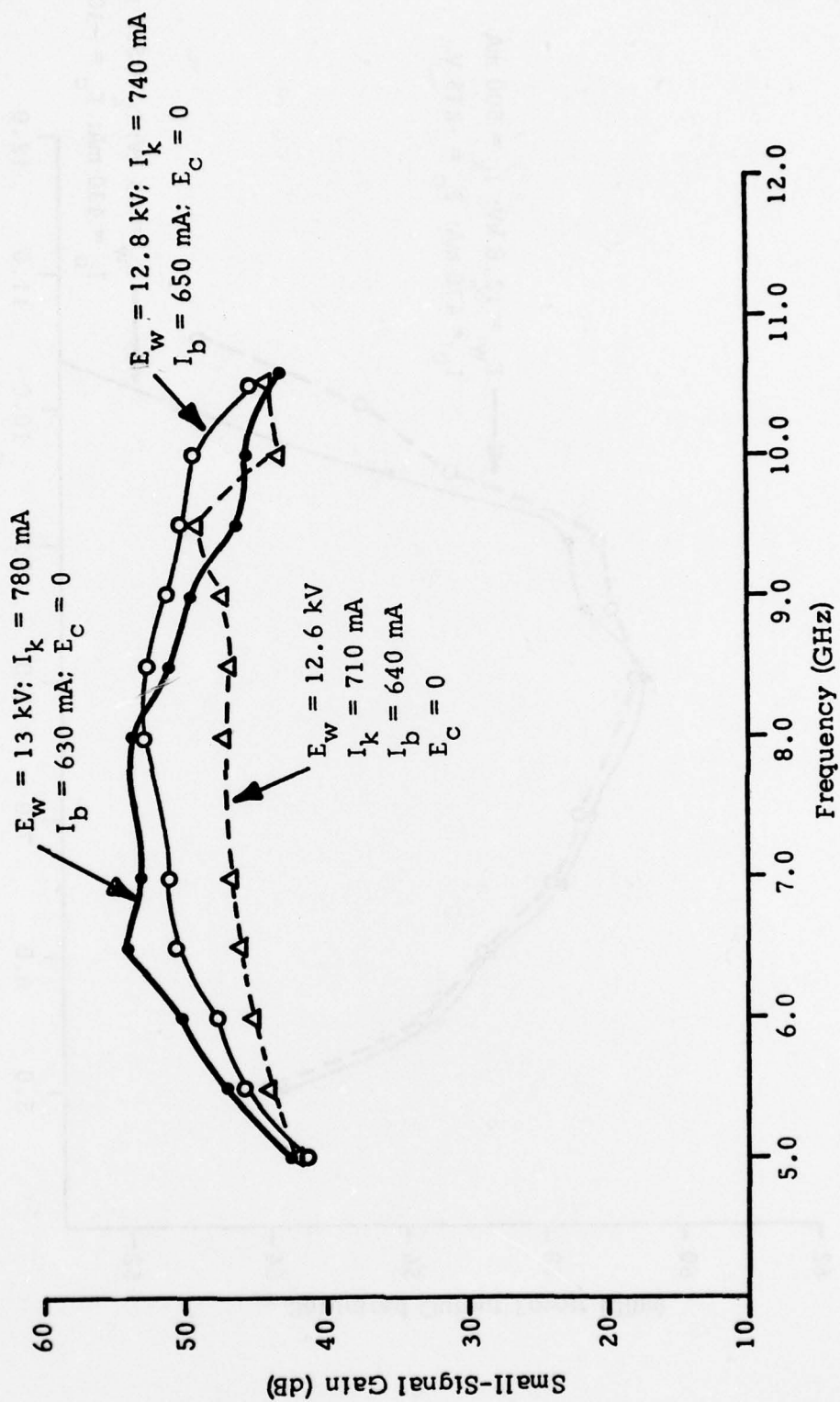
Figure 26. Small-signal gain for various helix voltages of tube SN 1.
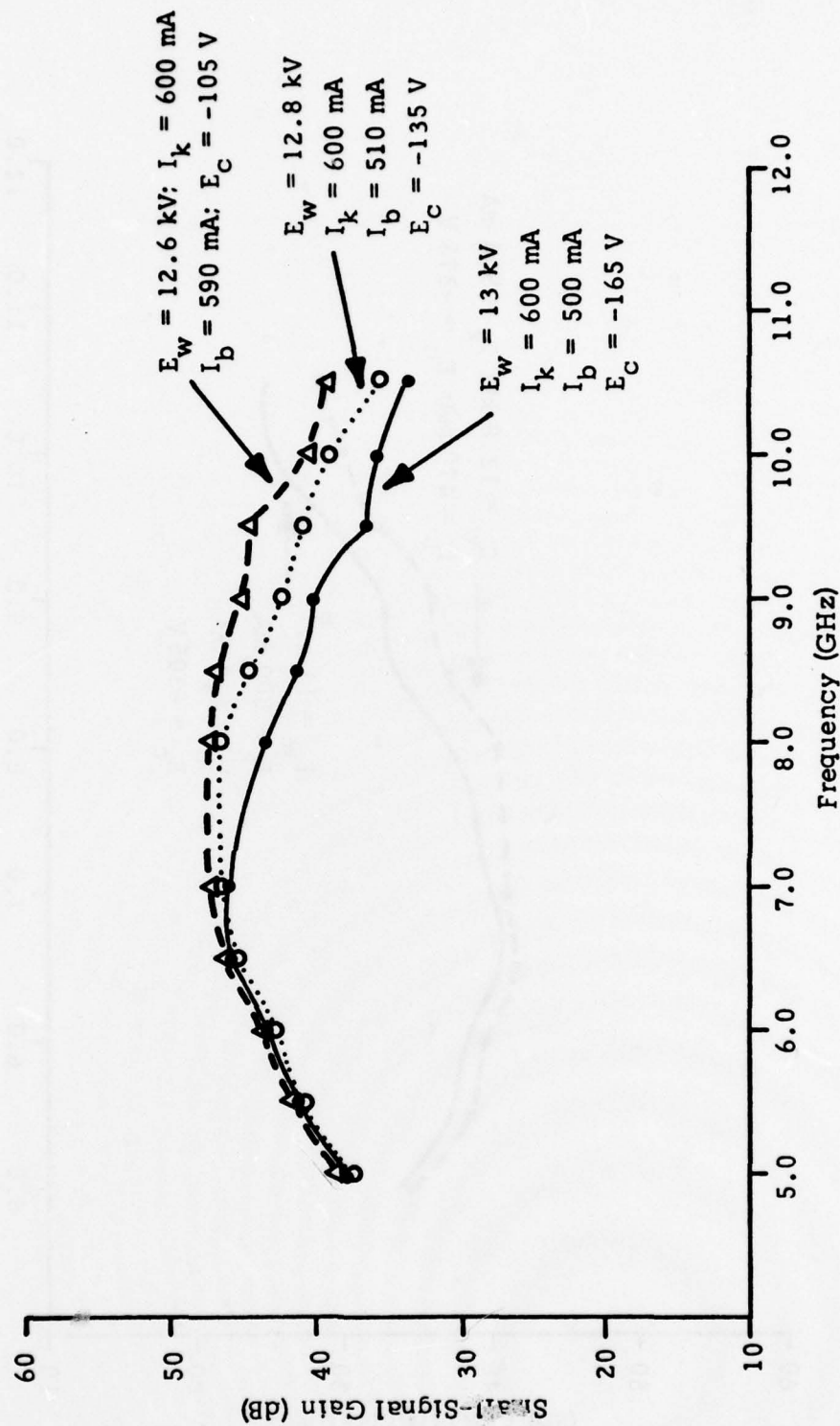
Figure 27. Small-signal gain at reduced beam currents for various helix voltages of tube SN 1.

-41-
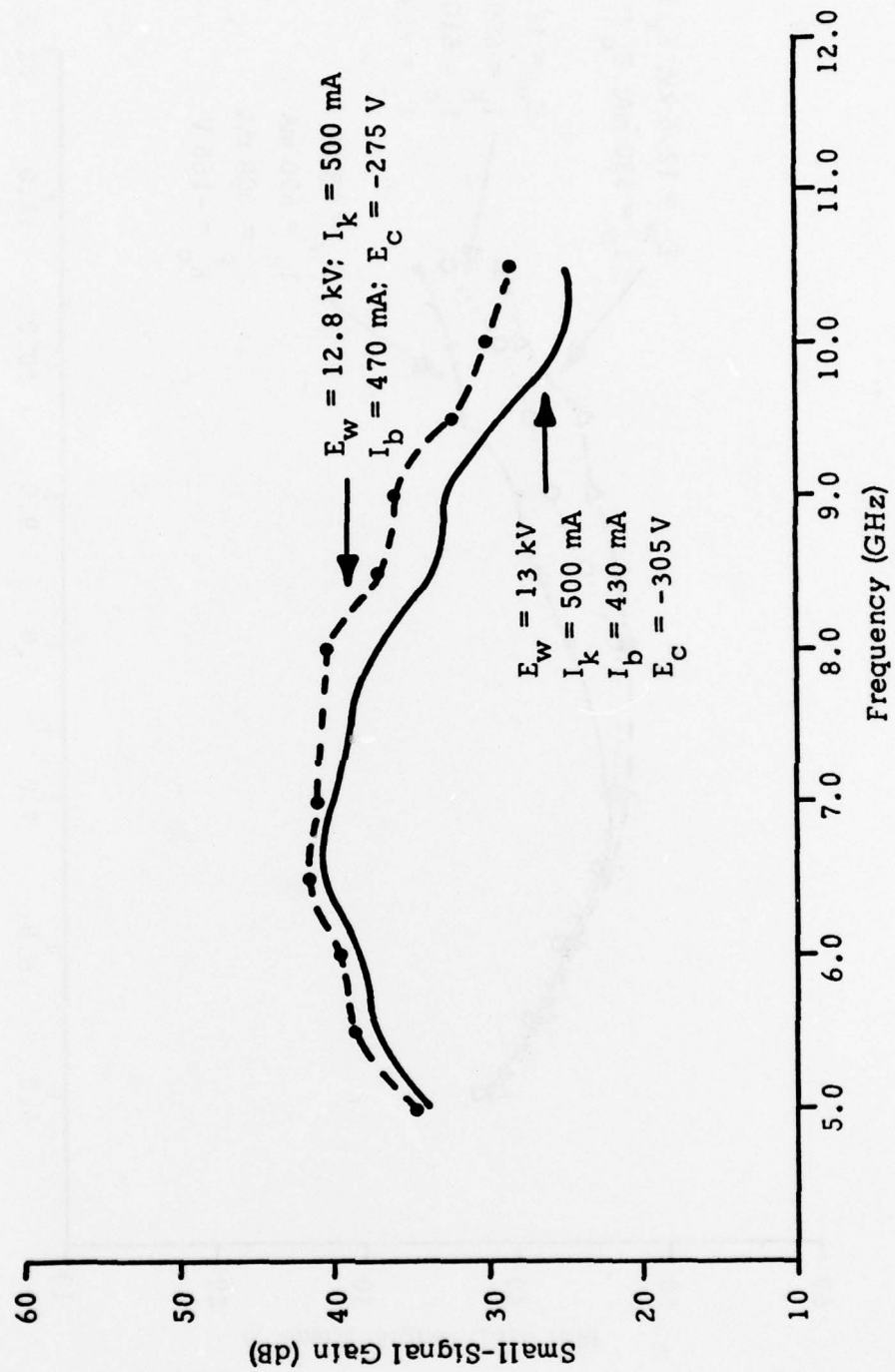
Figure 28. Small-signal gain at reduced beam currents for various helix voltages of tube SN 1.

-42-

Experiments were planned involving collector depression; they were not completed only as a result of a lack of equipment to operate the tube at higher duty.

6.0   PLANS

The work to be accomplished for the remainder of this program will be conducted according to the milestone plan shown in Figure 29.

Major efforts will be expended in the following areas:

- The first experimental tube of design A will be fully retested and evaluated when test equipments have been modified. Design B tubes will then be built and tested. Based on the results of designs A and B, a final experimental tube will be constructed with design upgrades in order to verify full RF performance.

- The mechanical design of the new three-stage collector will be improved for better voltage standoff, and the electrical design will be upgraded if necessary in an effort to achieve a collector efficiency of 52% in the pulse mode and 83% in the CW mode.

- The development of the new beryllia oxide window and waveguide transition will be accelerated so that they can be used on the final experimental tube.

- The scaled-up electron gun will be fully evaluated in the beam analyzer.

TASK	MONTH	AUG. '77				SEPT. '77					OCT. '77				NOV. '77				DEC. '77					JAN. '78			
	WK. ENDING	5	12	19	26	2	9	16	23	30	7	14	21	28	4	11	18	25	2	9	16	23	30	5	12	19	22
COLLECTOR DESIGN UPGRADE:																											
- MECHANICAL DESIGN FOR BETTER VOLTAGE STANDOFF		Δ	Δ																								
- ORDER NEW PARTS		Δ										Δ															
- BUILD NEW COLLECTORS													Δ		Δ												
GUN DESIGN:																											
- BUILD AND RE-EVALUATE NEW GUN IN BEAM ANALYZER		Δ	Δ																								
BeO WINDOW AND WAVEGUIDE TRANSITION DESIGN:																											
- CONTINUE BeO WINDOW BRAZING EXPERIMENTS								Δ																			
- DESIGN FIXTURES FOR MEASURING VSWR OF WAVEGUIDE TRANSITION & WINDOW - TO - HELIX JUNCTION		Δ																									
- ORDER FIXTURES		Δ					Δ																				
- CONDUCT MATCHING EXPERIMENTS												Δ															
PROTOTYPE VE's AND PACKAGE DESIGN:																											
- DESIGN FIXTURE FOR COPPER PLATED BARREL								Δ	Δ																		
- DESIGN PACKAGE																		Δ	Δ								
- ORDER PARTS											Δ BARREL		Δ						Δ PACKAGE		Δ						
BUILD & TEST TUBES:																											
- EVALUATE COMPLETE RF PERFORMANCE OF TUBE S/N 1			Δ																								
- EVALUATE COLLECTOR - DEPRESSION CHARACTERISTICS OF TUBE S/N 1 WHEN NEW MODULATOR IS AVAILABLE												Δ															
- BUILD & TEST DESIGN B TUBES (2 VE's)						Δ							Δ														
- BUILD & TEST FINAL DESIGN EXPERIMENTAL TUBES WITH COPPER PLATED OUTPUT BARRELS (2 VE'S)												Δ			Δ												
- BUILD & TEST PROTOTYPE TUBES (3 VE'S)																			Δ			Δ					
SHIP FINAL DESIGN TWT																											Δ

LEGEND: ORIGINAL START ○   REVISED START □   COMPLETED MILESTONE ○ □
ORIGINAL COMPLETE ▽   REVISED COMPLETE △   ▼ ▲

Figure 29. Milestone plan.